

LA-8452-MS

Informal Report

C.2 2

**SOLA-STAR:  
A One-Dimensional  
ICED-ALE Hydrodynamics Program for  
Spherically Symmetric Flows**

**DO NOT CIRCULATE**

**PERMANENT RETENTION**

**REQUIRED BY CONTRACT**

University of California



**LOS ALAMOS SCIENTIFIC LABORATORY**

Post Office Box 1663 Los Alamos, New Mexico 87545

This report was not edited by the Technical Information staff.

This work was supported by the US Department of Energy, Office of Basic Energy Sciences.

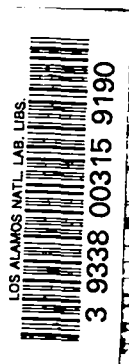
This report was prepared as an account of work sponsored by the United States Government. Neither the United States nor the United States Department of Energy, nor any of their employees, makes any warranty, express or implied, or assumes any legal liability or responsibility for the accuracy, completeness, or usefulness of any information, apparatus, product, or process disclosed, or represents that its use would not infringe privately owned rights. Reference herein to any specific commercial product, process, or service by trade name, mark, manufacturer, or otherwise, does not necessarily constitute or imply its endorsement, recommendation, or favoring by the United States Government or any agency thereof. The views and opinions of authors expressed herein do not necessarily state or reflect those of the United States Government or any agency thereof.

LA-8452-MS  
Informal Report

UC-34  
Issued: July 1980

**SOLA-STAR:  
A One-Dimensional  
ICED-ALE Hydrodynamics Program for  
Spherically Symmetric Flows**

L. D. Cloutman



SOLA-STAR: A ONE-DIMENSIONAL ICED-ALE HYDRODYNAMICS  
PROGRAM FOR SPHERICALLY SYMMETRIC FLOWS

by

L. D. Cloutman

ABSTRACT

This report describes a simple, general-purpose, and efficient algorithm for solving one-dimensional spherically symmetric, transient fluid-dynamics problems using a variation of the ICED-ALE technique. Included are the finite difference equations, three test problems that illustrate various capabilities of the program, and a complete code description, including a listing, sample data decks and output, a summary of important variable names, and hints for conversion to other operating systems.

---

I. INTRODUCTION

Several years ago we reported a technique for implementing the ICED-ALE methodology in a form suitable for numerically simulating a wide variety of spherically symmetric fluid flows.<sup>1</sup> An experimental computer program, VEGA, was written to test this methodology and was applied to the star formation problem. Although that technique was designed for astrophysical applications, it is by no means limited to them. In the interim, Group T-3 has developed the SOLA series of simplified numerical fluid dynamics programs<sup>2,3</sup> specifically for public distribution. In response to requests for copies of the VEGA program, we are presenting a simplified version, SOLA-STAR, in this report. This code follows the philosophy of the SOLA series inasmuch as the code is easy to understand and use, it can be used by persons with little numerical fluid dynamics experience, it is easily modified to include more complicated physics, and it is useful both as a teaching device and a serious research tool.

The numerical algorithm used in the present program is basically the same as reported in Ref. 1, so no derivation of the difference equations will be presented in this report. The derivation is based on a volume integration of the governing equations, and the interested reader can find the details in Refs. 1 and 4-6. The algorithm consists of two phases. Phase I is a partially implicit Lagrangian time step. In Phase II, the solution is rezoned (if desired) in a physically motivated manner that conserves mass, momentum, and internal energy. The only stability requirement is that

$$\frac{|u| \delta t}{\delta r} < 1 \quad (1)$$

everywhere on the mesh, where  $u$  is the velocity,  $\delta t$  is the time step, and  $\delta r$  is the width of a computational mesh cell. This limit requires that the fluid moves less than one cell width each computational cycle. Observance of this limit, proper choice of the donor cell parameter  $\alpha$  (to be described later), and choosing the time step such that no variable changes its value by more than some small amount, say 20%, has been sufficient to achieve numerical stability for all of the problems that we have run. A more detailed discussion of stability of the method (and of many other aspects of the method) can be found in Ref. 1.

## II. EQUATIONS FOR SPHERICALLY SYMMETRIC FLOWS

To simplify the program and minimize both computing time and core requirements, SOLA-STAR assumes a single-component ideal gas. The differential equations that we model are

$$\frac{\partial \rho}{\partial t} + \frac{1}{r^2} \frac{\partial}{\partial r} (r^2 \rho u) = 0 \quad , \quad (2)$$

$$\begin{aligned} \frac{\partial \rho u}{\partial t} + \frac{1}{r^2} \frac{\partial}{\partial r} (r^2 \rho u^2) = & - \rho g - \frac{\partial p}{\partial r} + \frac{1}{r^2} \frac{\partial}{\partial r} \left( r^2 (2\mu + \lambda) \frac{\partial u}{\partial r} \right) - \frac{2u(2\mu + \lambda)}{r^2} \\ & + \frac{2u}{r} \frac{\partial \lambda}{\partial r} \quad , \quad (3) \end{aligned}$$

and

$$\frac{\partial \rho I}{\partial t} + \frac{1}{r} \frac{\partial}{\partial r} (r^2 \rho u I) = -p \frac{1}{r} \frac{\partial}{\partial r} (r^2 u) + \frac{1}{r} \frac{\partial}{\partial r} \left( r^2 K \frac{\partial T}{\partial r} \right) + 2\mu \left[ \left( \frac{\partial u}{\partial r} \right)^2 + \frac{2u^2}{r^2} \right] + \lambda \left[ \frac{1}{r} \frac{\partial}{\partial r} (r^2 u) \right]^2, \quad (4)$$

where  $t$  is time,  $r$  is radius,  $\rho$  is the density,  $u$  is the radial velocity,  $p$  is the pressure,  $\mu$  is the coefficient of viscosity,  $\lambda$  is the second coefficient of viscosity,  $g$  is the gravitational acceleration,  $I$  is the specific internal energy,  $K$  is the conductivity, and  $T$  is the temperature. Normally we use

$$\lambda = -\frac{2}{3} \mu, \quad (5)$$

which is accurate for an ideal monatomic gas. If experimental values of  $\lambda$  are available for polyatomic gases, they can be used. However, the program will need modification. The gravitational acceleration is computed from a difference approximation to

$$g = \frac{4\pi G}{r} \int_0^r \rho x^2 dx, \quad (6)$$

where  $G$  is the gravitational constant. This procedure is more accurate than solution of the Poisson equation for the gravitational potential. The set of equations is closed by the equation of state, which we assume to be

$$p = (\gamma - 1) \rho I, \quad (7)$$

where  $\gamma$  is the ratio of specific heats.

### III. DIFFERENCE EQUATIONS

The SOLA-STAR difference equations are written in terms of the primitive variables  $p$ ,  $\rho$ ,  $I$ ,  $r$ , and  $u$ . Furthermore, simple averages are used to find values of variables at points other than those where they are defined. Transformations of variables are frequently advocated as a means of achieving better accuracy on a given computational mesh. However, as discussed in the SOLA-ICE report,<sup>3</sup> this approach has a number of disadvantages and pitfalls for general-purpose programs. First, it is much easier to create conservative difference schemes in the primitive variables. Second, transformations commonly introduce transcendental functions such as square roots and exponentials into the equations, and these functions are expensive to compute. Third, the transformed equations are usually more complicated, resulting in more debugging effort and increased execution time. Fourth, the transformation that gives the best accuracy is problem dependent and, in general, unknown. Heuristic arguments that lead to particular transformations are at best unreliable. Finally, if good resolution is used, all well-behaved transformations will give the same results as the primitive variables.

Advancement of the variables in time is accomplished in two phases. Phase I consists of a partially implicit Lagrangian time step, and Phase II consists of the rezoning procedure. The velocity is defined at cell edges, (or vertices) as shown in Fig. 1, and all other quantities are defined at cell centers.

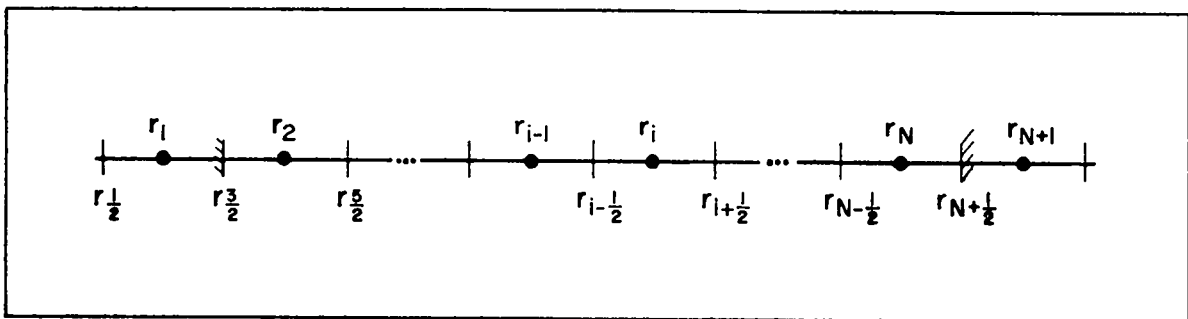


Fig. 1.

The SOLA-STAR computing mesh. Cell centers have integer subscripts, and cell edges have half-integer subscripts. We specify the cell edge positions and define the cell center positions by  $r_i = 0.5 * (r_{i+\frac{1}{2}} + r_{i-\frac{1}{2}})$ . Cells 1 and  $N+1$  are fictitious cells.

The spatial difference approximations for Phase I are derived by integrating the dynamical equations over a control volume taken to be a spherical shell coincident with the computational mesh. This procedure has been adequately described elsewhere,<sup>1,4,5,6</sup> so it will not be repeated here. The equations are written as fully implicit, and then they are made linear in the advanced time quantities. The linearization is illustrated by the equation of state:

$$p_j^{n+1} = (\gamma-1)_j^{n+1} \rho_j^{n+1} I_j^{n+1} \doteq (\gamma-1)_j^n \left( \rho_j^{n+1} I_j^n + \rho_j^n I_j^{n+1} - \rho_j^n I_j^n \right) \quad (8)$$

where the superscript denotes the time level, and the subscript denotes the spatial computational cell. We have computed protostellar models through central hydrogen dissociation and ionization (where the  $\gamma$  of the gas changes radically) with no sign of instability from the use of the explicit value of  $\gamma$ . In such a case we define  $\gamma$  not as the ratio of specific heats, but as  $\gamma-1 \equiv P/\rho I$ . The function  $\gamma-1$  is constant over much of the  $(\rho, T)$  plane, so a bilinear interpolation is accurate. In the regions of the  $(\rho, T)$  plane where  $(\gamma-1)$  is not constant, this interpolation scheme may be preferred over many of the higher order schemes advocated in the literature, including both second and third order polynomials and splines. Indiscriminant use of some of these schemes can introduce spurious oscillations into  $\gamma-1$ , leading to inaccurate numerical solutions.

Let us write the continuity equation as

$$\frac{d\rho}{dt} + \rho D = 0 \quad , \quad (9)$$

where

$$D = \frac{1}{r^2} \frac{\partial}{\partial r} (r^2 u) \quad . \quad (10)$$



Define the quantity

$$d_j^n = - \frac{\delta t}{1 + \delta t D_j^n} , \quad (11)$$

where

$$D_j^n = \frac{u_{j+\frac{1}{2}}^n - u_{j-\frac{1}{2}}^n}{r_{j+\frac{1}{2}} - r_{j-\frac{1}{2}}} + 2 \frac{u_{j+\frac{1}{2}}^n + u_{j-\frac{1}{2}}^n}{r_{j+\frac{1}{2}} + r_{j-\frac{1}{2}}} \quad (12)$$

Then Eq. (9) is approximated by

$$\rho_j^{n+1} - d_j^n \rho_j^n D_j^{n+1} = \rho_j^n , \quad (13)$$

which may be expanded to

$$\rho_j^{n+1} - u_{j+\frac{1}{2}}^{n+1} \rho_j^n d_j^n \left( \frac{2}{r_{j+\frac{1}{2}} + r_{j-\frac{1}{2}}} + \frac{1}{r_{j+\frac{1}{2}} - r_{j-\frac{1}{2}}} \right) - u_{j-\frac{1}{2}}^{n+1} \rho_j^n d_j^n \left( \frac{2}{r_{j+\frac{1}{2}} + r_{j-\frac{1}{2}}} - \frac{1}{r_{j+\frac{1}{2}} - r_{j-\frac{1}{2}}} \right) = \rho_j^n . \quad (14)$$

As with all our difference equations, the geometric quantities (that is,  $r$ ,  $A$ , and  $V$ ) are the old-time values. The left-hand side of Eq. (9) is differenced directly because the control volume integration procedure would provide no immediate information on new densities. It would merely give us the trivial fact that the mass in a cell does not change. The advanced-time cell volume, necessary to compute the advanced time density from the cell mass, is not directly available.

The equation for the specific internal energy may be written as

$$\frac{\partial \rho I}{\partial t} + \frac{1}{r} \frac{\partial}{\partial r} (r^2 \rho u I) = - p D + \frac{1}{r} \frac{\partial}{\partial r} \left( r^2 K \frac{\partial T}{\partial r} \right) + \Phi \quad (15)$$

For numerical reasons we have found it expedient to define the flux

$$F = K \frac{\partial T}{\partial r} = K \frac{\partial}{\partial r} \left( \frac{I}{c_v} \right) \quad (16)$$

and carry along this extra equation. For normal gases,  $K = \mu c_p / Pr$ , where  $Pr$  is the Prandtl number and  $c_p$  is the specific heat at constant pressure. For stellar problems where we are modeling radiation diffusion,  $K$  is the radiative conductivity. The quantity  $c_v$  is defined as  $I/T$ , so it is not always the usual specific heat. It is tabulated and treated numerically the same as  $\gamma-1$  for the general case. Incidentally, the turbulent conductivity defined by Eq. (28) of Ref. 1 did not work well and was replaced by an estimate based on the mixing length theory. The diffusion term in Eq. (15) is replaced by

$$\frac{1}{r} \frac{\partial}{\partial r} (r^2 F) \quad .$$

Carrying the additional flux equation is necessary wherever  $\chi \equiv \log_{10} (K \delta t / \rho c_v \delta r^2)$  approaches or exceeds the number of digits carried in the calculation, because the coefficient matrix has a term like  $1 + 2 \times 10^\chi$ . The one gets lost in round off if  $\chi$  is too large, and the matrix package cannot successfully recover the one in the course of solving the linear system.

The expression for the viscous dissipation term in Eq. (15) is

$$\phi \equiv 2\mu \left[ \left( \frac{\partial u}{\partial r} \right)^2 + \frac{2u^2}{r^2} \right] + \lambda \left[ \frac{1}{r^2} \frac{\partial}{\partial r} (r^2 u) \right]^2 . \quad (17)$$

The difference approximation to Eq. (15) is derived by integrating over the spherical shell between  $r = r_{j-\frac{1}{2}}$  and  $r = r_{j+\frac{1}{2}}$ , using the procedure described in Ref. 1. Define normalized cells volumes

$$V_{c,j} \equiv r_{j+\frac{1}{2}}^3 - r_{j-\frac{1}{2}}^3 , \quad (18)$$

and normalized vertex areas

$$A_{j-\frac{1}{2}} = 3r_{j-\frac{1}{2}}^2 . \quad (19)$$

Then

$$\begin{aligned} I_j^{n+1} = I_j^n + \delta t \left\{ \frac{V_{c,j}}{M_{c,j}} \phi_j + \frac{1}{M_{c,j}} \left[ A_{j+\frac{1}{2}} F_{j+\frac{1}{2}}^{n+1} - A_{j-\frac{1}{2}} F_{j-\frac{1}{2}}^{n+1} \right] \right. \\ \left. - \frac{1}{2M_{c,j}} \left[ p_j^{n+1} \left( A_{j+\frac{1}{2}} u_{j+\frac{1}{2}}^n - A_{j-\frac{1}{2}} u_{j-\frac{1}{2}}^n \right) + p_j^n \left( A_{j+\frac{1}{2}} u_{j+\frac{1}{2}}^{n+1} \right. \right. \right. \\ \left. \left. \left. - A_{j-\frac{1}{2}} u_{j-\frac{1}{2}}^{n+1} \right) \right] \right\} , \quad (20) \end{aligned}$$

where

$$M_{c,j}^n = \rho_j^n v_{c,j} \quad , \quad (21)$$

and

$$\begin{aligned} \phi_j = & \mu_j^n \left\{ 2 \left[ 2 \left( u_{j+\frac{1}{2}}^{n+1} - u_{j-\frac{1}{2}}^{n+1} \right) \left( u_{j+\frac{1}{2}}^n - u_{j-\frac{1}{2}}^n \right) - \left( u_{j+\frac{1}{2}}^n - u_{j-\frac{1}{2}}^n \right)^2 \right] \left( r_{j+\frac{1}{2}} - r_{j-\frac{1}{2}} \right)^{-2} \right. \\ & + 2 \left[ 4 \left( u_{j+\frac{1}{2}}^{n+1} + u_{j-\frac{1}{2}}^{n+1} \right) \left( u_{j+\frac{1}{2}}^n + u_{j-\frac{1}{2}}^n \right) - 2 \left( u_{j+\frac{1}{2}}^n + u_{j-\frac{1}{2}}^n \right)^2 \right] \left( r_{j+\frac{1}{2}} + r_{j-\frac{1}{2}} \right)^{-2} \\ & - \frac{2}{3(v_{c,j})^2} \left[ 2 \left( A_{j+\frac{1}{2}} u_{j+\frac{1}{2}}^{n+1} - A_{j-\frac{1}{2}} u_{j-\frac{1}{2}}^{n+1} \right) \left( A_{j+\frac{1}{2}} u_{j+\frac{1}{2}}^n - A_{j-\frac{1}{2}} u_{j-\frac{1}{2}}^n \right) \right. \\ & \left. \left. - \left( A_{j+\frac{1}{2}} u_{j+\frac{1}{2}}^n - A_{j-\frac{1}{2}} u_{j-\frac{1}{2}}^n \right)^2 \right] \right\} . \quad (22) \end{aligned}$$

The viscous dissipation term is positive-definite if all velocities are at the same time level, but we lose this physical characteristic by using velocities from a mixture of time levels. This is probably not serious, but it should be noted.

The flux equation is

$$F_{j+\frac{1}{2}}^{n+1} = \frac{2K_{j+\frac{1}{2}}^n}{r_{j+2/3} - r_{j-\frac{1}{2}}} \left( \frac{I_{j+1}^{n+1}}{c_{v,j+1}^n} - \frac{I_j^{n+1}}{c_{v,j}^n} \right) . \quad (23)$$

The momentum equation is given by

$$\begin{aligned} \frac{\partial \rho u}{\partial t} + \frac{1}{r} \frac{\partial}{\partial r} (r^2 \rho u^2) = & - \rho g - \frac{\partial p}{\partial r} + \frac{1}{r} \frac{\partial}{\partial r} \left[ r^2 (2\mu + \lambda) \frac{\partial u}{\partial r} \right] \\ & - \frac{2u(2\mu + \lambda)}{r} + \frac{2u}{r} \frac{\partial \lambda}{\partial r} . \quad (24) \end{aligned}$$

The Lagrangian form of Eq. (24) is differenced by integrating over a spherical shell (momentum control volume) between  $r_{j-1} = 0.5(r_{j-3/2} + r_{j-1/2})$  and  $r_j = 0.5(r_{j+1/2} + r_{j-1/2})$ .

$$\begin{aligned}
\frac{M_{v,j-1/2}^n}{\delta t} (u_{j-1/2}^{n+1} - u_{j-1/2}^n) &= -M_{v,j-1/2}^n g_{j-1/2} - 2V_{v,j-1/2} \frac{(p_j^{n+1} - p_{j-1}^{n+1})}{r_{j+1/2} - r_{j-3/2}} \\
&+ \frac{4}{3} \left[ A_j u_j^n \frac{u_{j+1/2}^{n+1} - u_{j-1/2}^{n+1}}{r_{j+1/2} - r_{j-1/2}} \right. \\
&- \left. A_{j-1} \mu_{j-1}^n \frac{u_{j-1/2}^{n+1} - u_{j-3/2}^{n+1}}{r_{j-1/2} - r_{j-3/2}} \right] \\
&- \frac{4}{3} V_{v,j-1/2} \left[ \frac{u_{j-1/2}^{n+1}}{r_{j-1/2}} 2 \left( \frac{\mu_j^n - \mu_{j-1}^n}{r_{j+1/2} - r_{j-3/2}} \right. \right. \\
&\left. \left. + \frac{\mu_j^n + \mu_{j-1}^n}{r_{j-1/2}} \right) \right], \tag{25}
\end{aligned}$$

where the vertex masses and vertex volumes are given by

$$M_{v,j-1/2} = (M_{c,j} + M_{c,j-1})/2, \tag{26}$$

$$V_{v,j-1/2} = r_j^3 - r_{j-1}^3. \tag{27}$$

The shell areas,  $A_j$ , are defined at cell centers, as indicated by the integral subscripts. To obtain the gravitational acceleration, we perform the sum

$$g_{j-1/2} = \frac{4\pi G}{3r_{j-1/2}^2} \sum_{i=2}^{j-1} M_{c,i}. \tag{28}$$

The equations form a banded linear system in the advanced time quantities, so they may be solved by a banded matrix package, such as the one by Hindmarsh.<sup>7</sup> The left element of each row of the band is stored in the computer with an index of 1. A simple mnemonic display of the subscripting scheme is given in the program listing in Appendix A.

In Phase II we are modeling the convection term

$$\iint_S \rho Q (\underline{u}_g - \tilde{u}) \cdot \hat{n} ds \quad , \quad (29)$$

where  $\underline{u}_g$  is the grid velocity and  $\tilde{u}$  is the fluid velocity at the end of Phase I. We define the difference velocity for our one-dimensional problems,  $w_{j-\frac{1}{2}} \equiv u_{g,j-\frac{1}{2}} - \tilde{u}_{j-\frac{1}{2}}$ , which is the velocity of the mesh relative to the fluid. Then  $w_{j-\frac{1}{2}} A_{j-\frac{1}{2}} \delta t$  is the volume relative to the fluid that is swept out by the moving grid point. One might be tempted to take for, say the density, simply an average of the densities on either side of the moving mesh point. This is called centered differencing, and it is unstable. For this reason we use a mixture of centered differencing and donor cell differencing. The donor cell component adds a strong stabilizing diffusional truncation error that compensates for the destabilizing diffusional error of centered differencing.

Define the donor cell parameter,  $\alpha_{j+\frac{1}{2}}$ , by

$$\alpha_{j+\frac{1}{2}} = -\bar{\alpha} \operatorname{sgn}(w_{j+\frac{1}{2}}) \quad , \quad (30)$$

where the function  $\operatorname{sgn}$  is the sign of the argument, and  $\bar{\alpha}$  is a constant,  $0 \leq \bar{\alpha} \leq 1$ . As an example of the difference form of the convection term for a cell centered quantity,

$$M_{c,j}^{n+1} = M_{c,j}^n - \frac{\delta t}{2} \left\{ w_{j-\frac{1}{2}} A_{j-\frac{1}{2}} \left[ (1 + \alpha_{j-\frac{1}{2}}) \tilde{\rho}_{j-1} + (1 - \alpha_{j-\frac{1}{2}}) \tilde{\rho}_j \right] - w_{j+\frac{1}{2}} A_{j+\frac{1}{2}} \left[ (1 + \alpha_{j+\frac{1}{2}}) \tilde{\rho}_j + (1 - \alpha_{j+\frac{1}{2}}) \tilde{\rho}_{j+1} \right] \right\} \quad . \quad (31)$$

The tildes denote results from Phase I. This is a straightforward approximation to Eq. (29) for  $Q = 1$ . The density is obtained by calculating volumes from the new mesh position

$$r_{j-\frac{1}{2}}^{n+1} = r_{j-\frac{1}{2}}^n + u_{g,j-\frac{1}{2}} \delta t \quad . \quad (32)$$

Then

$$\rho_j^{n+1} = \frac{M_{c,j}^{n+1}}{V_{c,j}^{n+1}} \quad , \quad (33)$$

which ensures mass conservation. The convection of internal energy is handled in exactly the same manner.

For momentum the control volume runs from cell center to cell center, and a slight modification is necessary. The difference velocity must be obtained by averaging the difference velocities of the neighboring vertices. This leads to

$$\begin{aligned} u_{j-\frac{1}{2}}^{n+1} = \frac{1}{M_{v,j-\frac{1}{2}}^{n+1}} & \left\{ M_{v,j-\frac{1}{2}}^n u_{j-\frac{1}{2}}^n - \frac{\delta t}{4} \left[ \tilde{\rho}_{j-1} (w_{j-\frac{1}{2}} + w_{j-3/2}) A_{j-1} \left( (1+\alpha_{j-1}) \tilde{u}_{j-3/2} \right. \right. \right. \\ & + (1-\alpha_{j-1}) \tilde{u}_{j-\frac{1}{2}} \left. \left. \left. \right) - \tilde{\rho}_j (w_{j-\frac{1}{2}} + w_{j+\frac{1}{2}}) A_j \left( (1+\alpha_j) \tilde{u}_{j-\frac{1}{2}} \right. \right. \right. \\ & \left. \left. \left. + (1-\alpha_j) \tilde{u}_{j+\frac{1}{2}} \right) \right] \right\} \quad , \quad (34) \end{aligned}$$

where

$$\alpha_j = -\bar{\alpha} \operatorname{sgn} (w_{j-\frac{1}{2}} + w_{j+\frac{1}{2}}) \quad . \quad (35)$$

It is not necessary to use the same  $\bar{\alpha}$  in the momentum equation as in the equation for the mass or energy. We have found empirically that we need more donor cell in the mass and energy equations to keep cells from emptying out in the neighborhood of steep gradients.

For problems with strong shocks, an explicit artificial viscous pressure is helpful in attaining numerical stability and accurate jump conditions. The form we have chosen is

$$q_j^n = - \Lambda \rho_j^n (x_{j+\frac{1}{2}} - x_{j-\frac{1}{2}})^2 D_j^n \min(0, D_j^n) \quad , \quad (36)$$

where  $\Lambda$  is a constant of order unity. To the right side of Eq. (20), we add  $-\delta t q_j^n D_j^n$ . To the right side of Eq. (25), we add  $2V_{v,j-\frac{1}{2}} (q_{j-1}^n - q_j^n) / (r_{j+\frac{1}{2}} - r_{j-\frac{3}{2}})$ . In regions of expansion,  $q$  vanishes. In regions of compression, the  $q$  terms provide velocity diffusion in the momentum equation and "viscous" conversion of kinetic energy to thermal energy in the I equation. These terms have an effective kinematic viscosity that is roughly the fluid velocity times a mesh cell size in the neighborhood of a shock. The artificial viscous effects are concentrated in the regions of strongest compression, precisely where they are needed the most. For problems with no shocks,  $\Lambda = 0$  is recommended.

#### IV. NUMERICAL EXAMPLES

This section contains three numerical examples that illustrate the kinds of problems that may be solved with SOLA-STAR. The first example provides a test problem to be used to check out new copies of the code. These examples are crude simulations of physical problems, and are not intended to be compared to observations without some refinement. The first problem is the early collapse phase of a protostellar cloud. This is basically the same problem solved by Larson.<sup>8</sup> The second test problem is a simple blast wave for which there is an analytical solution. The third problem is the solar wind solution by Hundhausen and Gentry.<sup>9</sup> They considered the effects of transients imposed on a steady state solar wind.

##### A. Collapse Of a Protostellar Cloud

The first numerical fluid dynamics calculation of the collapse of a dense interstellar cloud to form a protostar was published by Larson.<sup>8</sup> His initial condition was an isothermal cloud of uniform density that was just unstable toward gravitational collapse according to the Jeans criterion. The outer boundary condition was  $u=0$  at just under the Jeans' radius. Larson's solution for a one solar mass cloud was confirmed by Ruppel and Cloutman,<sup>1</sup> and the results



presented in this subsection and the code listing and output in Appendix A are for a similar one solar mass cloud.

Since some results of VEGA calculations were described fully and compared to Larson's results in reference 1, we will limit the present discussion to the use of this problem as a test case for new copies of the program. Appendix A provides the actual computer output at 0, 1, 500, and 3000 cycles. The following physical events can be seen in the solution as it develops. First, a rarefaction is created at the outer boundary at  $t = 0$  by the collapse of the cloud. It travels inward at the speed of sound. The density is spatially constant but temporally increasing inside the rarefaction, and it falls off as  $1/r^2$  outside. This behavior is illustrated in figure 2 with the curve from cycle 300 ( $t = 2.981 \times 10^{12}$  s). The velocity profile consists of two linear segments with the minimum at the rarefaction, as illustrated in figure 3. The material is isothermal at 10 K. When the rarefaction reaches the center, the embryonic star is formed. The density becomes peaked at the center, forming a body nearly in hydrostatic equilibrium, surrounded by an accretion shock. The central body contains roughly  $10^{-3}$  solar masses and has a radius of about  $10^{14}$  cm. Upon its creation, the protostar may oscillate briefly. Cloud material falls supersonically to the accretion shock, is decelerated, and added to the protostar. The central density continues to rise. When it reaches about  $10^{-13}$  g/cm<sup>3</sup>, the central temperature also begins to rise. This phase is illustrated in figures 2 and 3 with the curves from cycle 900 ( $t = 8.578 \times 10^{12}$  s). When the central temperature reaches 2000 K, the calculation is terminated. Figure 4 shows the structure at 3500 cycles ( $t = 8.653 \times 10^{12}$  s), shortly before termination. Real gas physics is needed to go farther because of the importance of H<sub>2</sub> dissociation. This has been done in VEGA by making tables of  $(\gamma-1) \equiv p/\rho I$  and  $c \equiv I/T$  using the equation of state in Paczynski's stellar envelope program.<sup>10v</sup> This pseudo- $\gamma$  and pseudo-specific heat are easy to insert into the code, and they need to be evaluated only at time level  $n$  for use in the coefficient matrix. In addition, they are constant over large parts of the  $\rho$ - $T$  plane, so bilinear interpolation is sufficiently accurate.

### B. Spherical Blast Wave

The spherical blast wave is a classical test problem for numerical fluid dynamics codes, and it is a much more severe test than piston-driven shocks or shock tubes. In these latter cases, the solutions are piece-wise constant except for the expansion wave in a shock tube, which generally has only modest

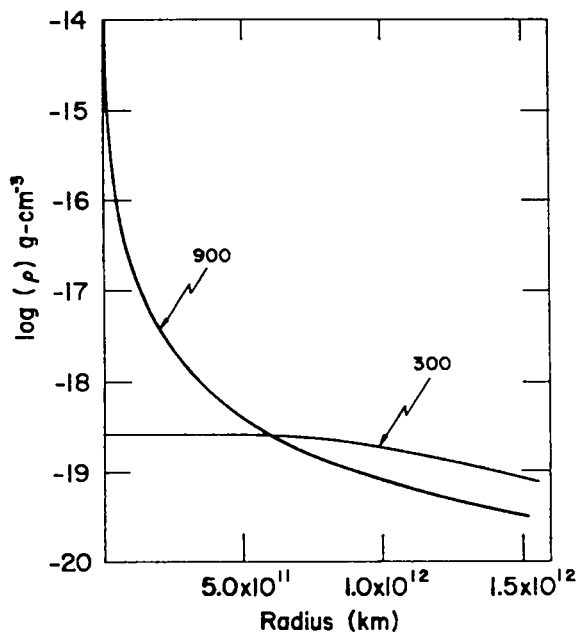


Fig. 2.  
Runs of density at cycles 300 and 900  
in the protostar calculation.

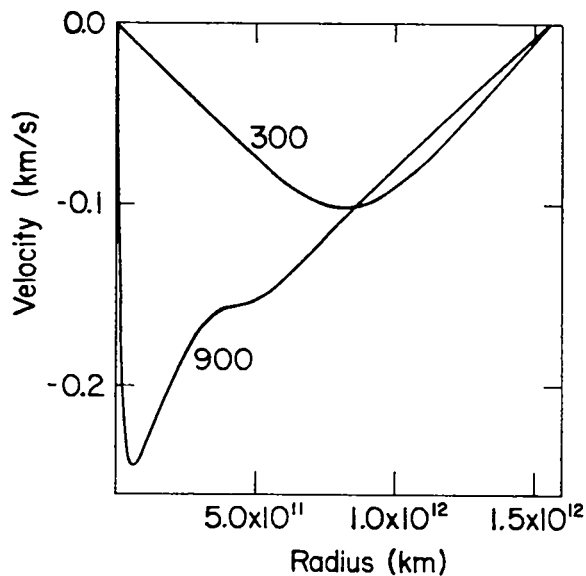


Fig. 3.  
Runs of velocity at 300 and 900 cycles  
in the protostar calculation.

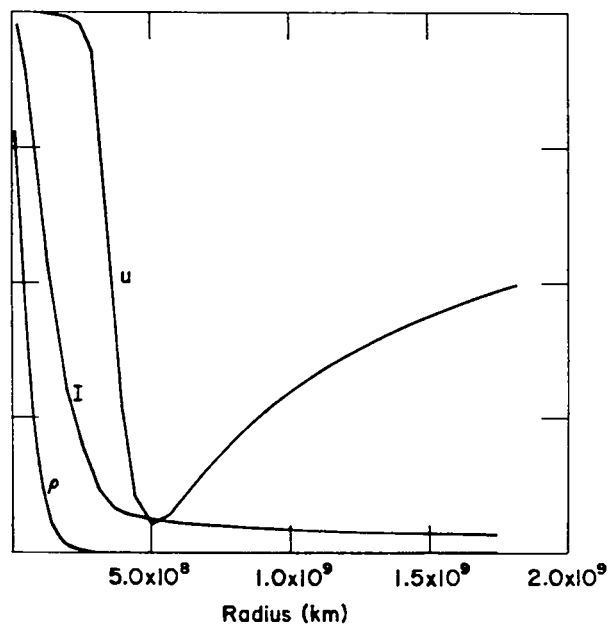


Fig. 4.  
The protostar solution at 3500 cycles.  
The vertical axis runs from  $-3 \times 10^5$   
to  $0 \text{ cm-s}^{-1}$  for the radial velocity ( $u$ ),  
 $0$  to  $1.5 \times 10^{-8} \text{ g-cm}^{-3}$  for the density  
( $\rho$ ), and  $0$  to  $10^{11}$  for the specific in-  
ternal energy ( $I$ ).

curvature. On the other hand, the blast wave solution is sharply peaked, presenting a real challenge for finite difference methods.

The sample problem discussed in this section is based on a  $10^{51}$  erg point explosion in a 10,000 K and  $\rho = 2.4 \times 10^{-9}$  g/cm<sup>3</sup> ambient medium with  $\gamma = 5/3$ . Appendix B gives UPDATE modifications and the data deck.

Figure 5 shows the numerical solution for the density at two different times. The solid curves are for  $\alpha = 1.0$  (pure donor cell transport) and the dashed curve is for  $\alpha = 0.6$ . Note that decreasing  $\alpha$  reduces the numerical diffusion, thereby sharpening the peaks. Note also the improvement in the density jump condition as the wave progresses. This is due to two phenomena. First, the initial condition is not the Taylor-Sedov solution, toward which the solution evolves. Second, and more importantly, the resolution of the sharp self-similar peak improves as the radius of the shock grows to include more cells.

### C. Solar Wind

A simple solar wind model is presented to illustrate use of the code with inflow and outflow boundaries. It also has the left-most vertex away from the

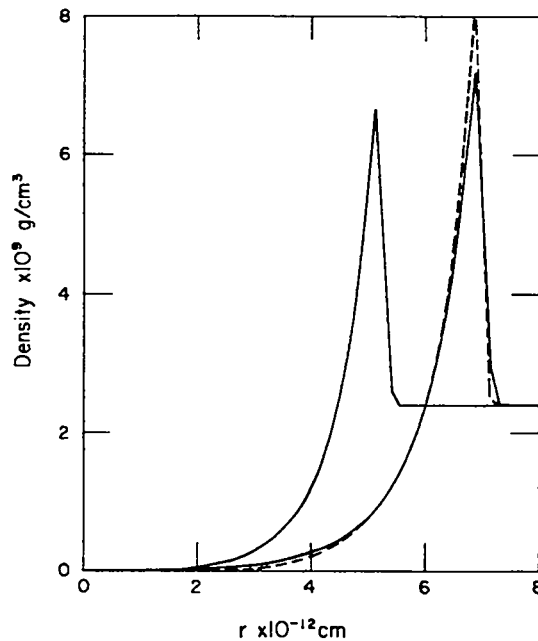


Fig. 5.

Runs of density for blast wave solutions. The solid curves are for  $\alpha = 1.0$  at 150 cycles ( $t = 96.5$  s) and 300 cycles ( $t = 216.5$  s). The dashed curve is for  $\alpha = 0.6$  at 300 cycles ( $t = 212.3$  s). The peak of the analytical solution is  $9.6 \times 10^{-9}$  g cm<sup>-3</sup> at  $r = 7.2 \times 10^{12}$  cm at 300 cycles.

origin. This feature is also useful for running a Cartesian problem merely by making X(2) much larger than the total width of the mesh.

The sample solutions presented here are repetitions of solutions by Hundhausen and Gentry (HG).<sup>9</sup> The first step in this problem is to find a steady state solar wind solution. This could be accomplished by letting the program go through a transient phase. However, the computational effort was minimized by using an inviscid analytical solution as the initial condition. Then transient disturbances were introduced into the solution to represent perturbations by solar flares, and their propagation was followed.

The initial condition is an inviscid adiabatic radial expansion of an ideal gas:

$$p = (\gamma-1)\rho I = C_1 \rho^\gamma \quad , \quad (37)$$

$$r^2 \rho u = C_2 \quad , \quad (38)$$

and

$$u \frac{du}{dr} + \frac{1}{\rho} \frac{dp}{dr} + \frac{GM}{r^2} = 0 \quad , \quad (39)$$

where M is the mass of the sun. Substituting (37) into (39) and integrating, we find

$$I + \frac{1}{2} u^2 + \frac{p}{\rho} - \frac{GM}{r} = C_3 \quad , \quad (40)$$

which is the Bernoulli equation for this problem. The constants  $C_1$ ,  $C_2$ , and  $C_3$  are evaluated by specifying the values of all variables at  $r = 1.25 \times 10^{12}$  cm, which is outside the critical point of the inviscid solar wind. Elimination of all dependent variables except  $\rho$  leads to a transcendental equation for  $\rho$ :

$$\rho^2 \left( C_3 + \frac{GM}{r} - \frac{\gamma C_1}{\gamma-1} \rho^{\gamma-1} \right) = \frac{C_2^2}{2r^4} \quad (41)$$

This form is solved iteratively by the program, and then the other variables are found trivially by using equations (37) and (38).

The inflow boundary at the left is straightforward, as can be seen from the UPDATE modifications given in the appendix C. However, outflow boundaries are always more troublesome. One simple form that is frequently useful is the continuative boundary, where all gradients are set to zero on the boundary. This procedure is often adequate for supersonic flows, but can reflect unwanted signals into the mesh for subsonic flows. We use an alternate approach, the radiation condition

$$\frac{\partial c}{\partial t} + u \frac{\partial c}{\partial r} = 0 \quad , \quad (42)$$

where  $c$  is one of the flow variables, in place of the continuative boundary. A small bump in the velocity at the right end of the mesh is strictly a numerical artifact of the outflow boundary. It is slightly smaller using equation (42) than the continuative boundary, and the supersonic outflow prevents it from propagating into the mesh. The user may have to develop a better outflow boundary condition for some problems.

The first numerical solution we ran was the generation of a steady state solution. The analytic solution from equations (37), (38), and (41) was used as the initial condition. The parameters of HG were used. The problem was run beyond the time it takes an element of fluid to cross the mesh, and the numerical and analytic steady states were compared. During the transient, the interface between the fluid originally in the mesh and the fluid that subsequently flowed into the mesh propagated to the right, showing a small disturbance of increasing amplitude that exited the mesh without reflection. Comparison of the computer-generated plots shows the analytic and computational solutions are almost indistinguishable. Examination of the numerical output shows that the worst errors are near the left boundary where gradients of the variables are the largest. The mesh has been compressed in this region to reduce the error, which has a maximum of 4% in the pressure. The other variables are computed more accurately, and the accuracy of all variables improves at larger  $r$ .

The second numerical solution was the same as the transient shock problem solved by HG. A disturbance lasting 2.1 hours was introduced into the mesh at

$t_0 = 2 \times 10^5$  s. This initial period was introduced to allow the inner boundary perturbation to propagate well into the mesh where it could be ignored. This procedure is probably not necessary. Figure (6) corresponds to figures (1)-(3) of HG, and the interested reader is invited to compare the results. The top row of figure 6 shows the solution at 2.0 hrs. after  $t_0$ . The analytical solution has a velocity of 1570 km/s just behind the shock, in good agreement with our calculation. The velocity jump in HG's figure 1 is a bit too high. Our velocity profile has a spike behind the shock. As we are running with  $\alpha = 0.5$ , this feature is probably a dispersive truncation error. HG show no spike, suggesting that perhaps their solution was obtained using full donor cell transport ( $\alpha = 1$ ). However, Gentry (private communication) has pointed out that at least part of the HG work was done with a scheme that was more closely related to the truncation error cancellation technique of Rivard and collaborators,<sup>11</sup> which is similar in principle to locally computing and applying the minimum  $\alpha$  needed in each cell to get numerical stability. This procedure often allows significant dispersive errors to occur, especially near a strong shock, so it is not clear what differencing scheme HG used to obtain their published results.

An unexpected feature of the numerical solutions is the density jump across the shock. The analytic value is a factor of four. Our solution gives a factor of seven, and HG's jump is about the same in spite of the label on their graph showing good agreement with a factor of four jump. The explanation may be that the density gradient is quite large in this region, so shocked material compressed by the correct amount is more than four times as dense as the material ahead of the shock, several cells away.

The second row of figure 6 is taken at  $t_0 + 4.3$  hr. The agreement with HG is better than at  $t_0 + 2.1$  hr, especially in the velocity field. The density jump in the SOLA-STAR solution is still apparently a bit higher than expected.

The bottom row of figure 6 was taken at  $t_0 + 20.1$  hr, as was HG's figure 3. HG's velocity curve is slightly broader and smoother. Their density jump and ours now are close to the desired factor of four, but the velocity and density profiles differ somewhat in detail. Although our solution is in qualitative agreement with that of HG, it is clear that some unanswered questions about these solar wind solutions remain.

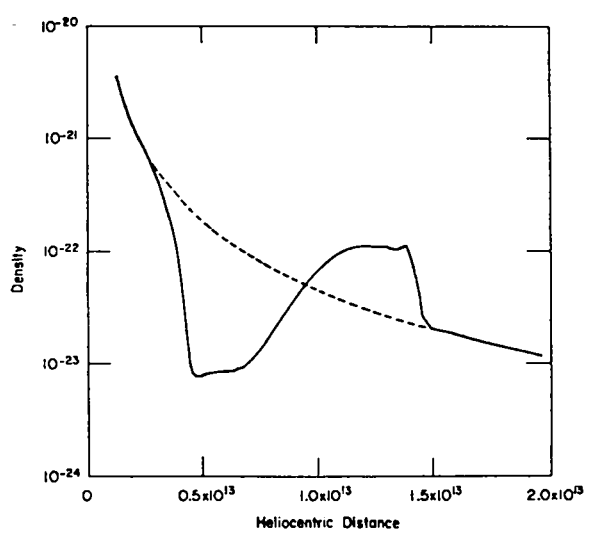
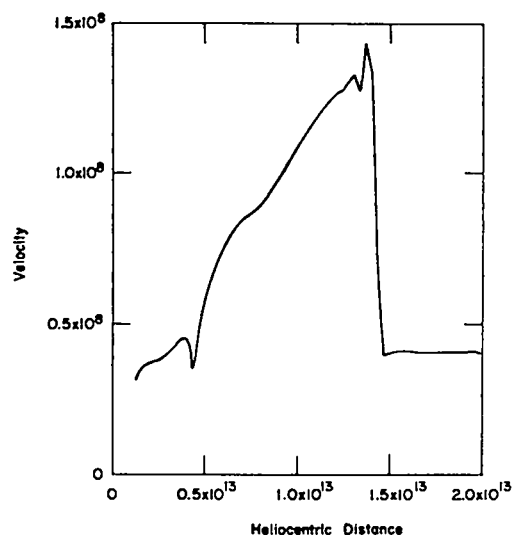
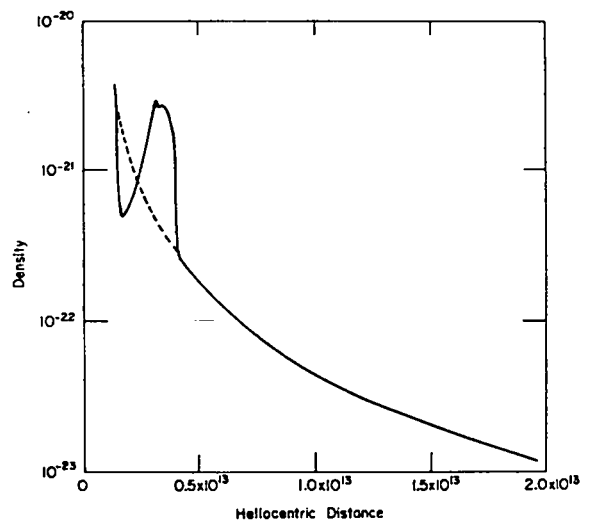
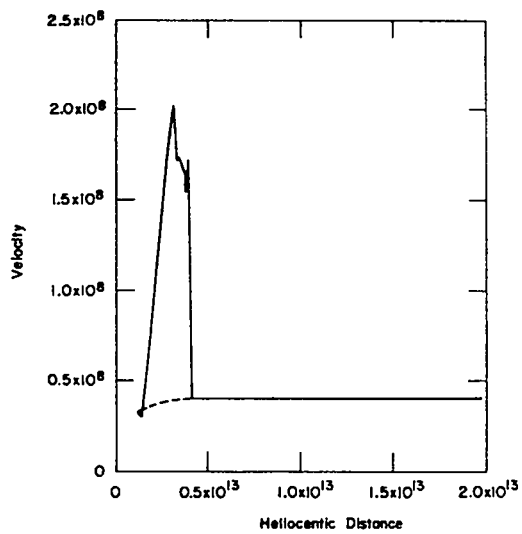
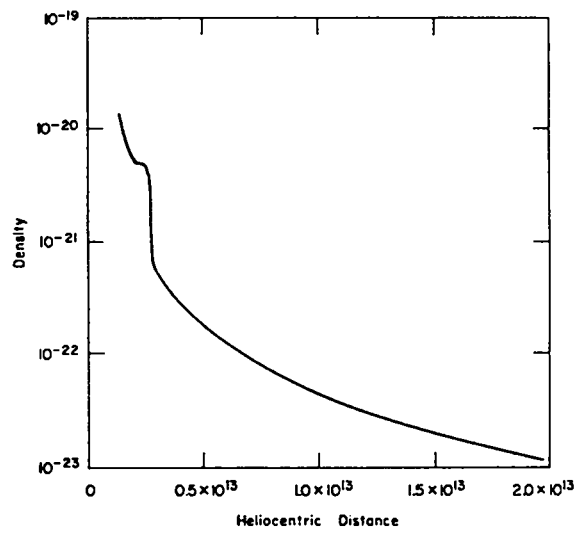
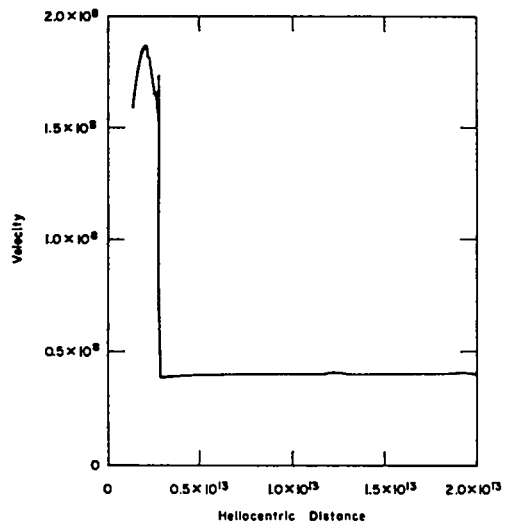


Fig. 6.

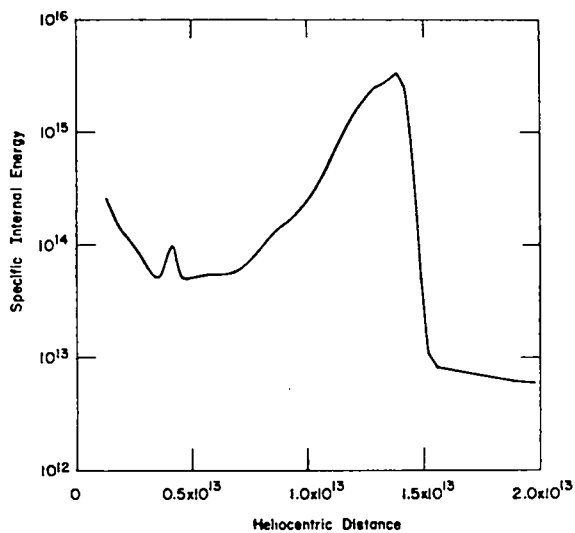
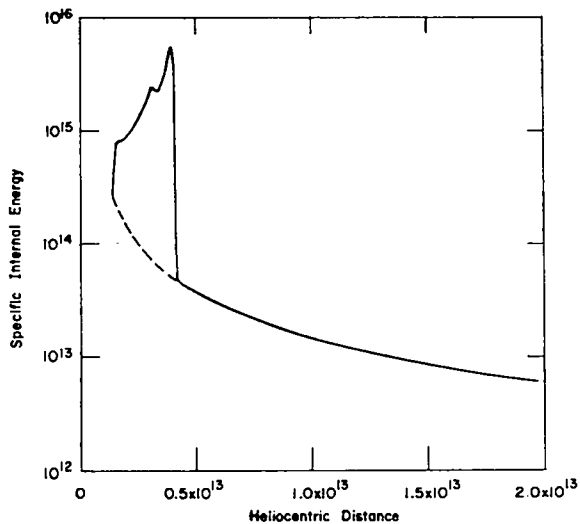
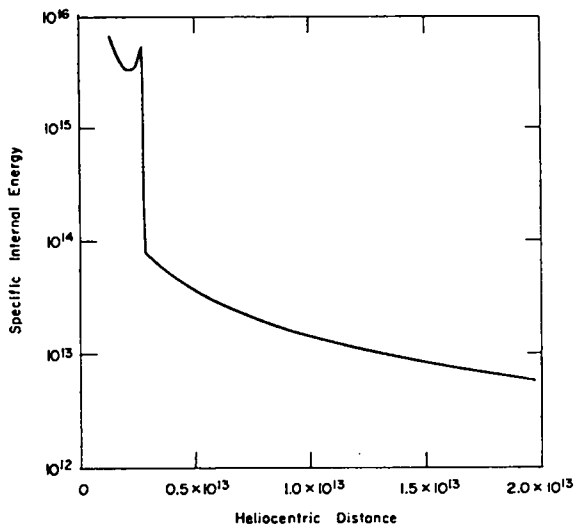


Fig. 6 (con't)  
 The solar wind solution at 2.0 hr.,  
 4.3 hr., and 20.1 hr. after beginning  
 the shock wave inflow for the top,  
 middle, and bottom rows of figures re-  
 spectively. Dashed lines indicate the  
 steady state solar wind.



## REFERENCES

1. Ruppel, H. M. and Cloutman, L. D., "A General Numerical Fluid Dynamics Algorithm for Astrophysical Applications," Los Alamos Scientific Laboratory report LA-6149-MS (1975).
2. Hirt, C. W., Nichols, B. D., and Romero, N. C., "SOLA - A Numerical Solution Algorithm for Transient Fluid Flows," Los Alamos Scientific Laboratory report LA-5852 (1975).
3. Cloutman, L. D., Hirt, C. W., and Romero, N. C., "SOLA-ICE: A Numerical Solution Algorithm for Transient Compressible Fluid Flows," Los Alamos Scientific Laboratory report LA-6236 (1976).
4. Hirt, C. W., Amsden, A. A., and Cook, J. L., "An Arbitrary Lagrangian-Eulerian Computing Method for All Flow Speeds," J. Comp. Phys., 14, 227 (1974).
5. Amsden, A. A. and Hirt, C. W., "YAQUI: An Arbitrary Lagrangian-Eulerian Computer Program for Fluid Flow at All Speeds," Los Alamos Scientific Laboratory report LA-5100 (1973).
6. Butler, T. D., Cloutman, L. D., Dukowicz, J. K., and Ramshaw, J. D., "CONCHAS: An Arbitrary Lagrangian-Eulerian Computer Code for Multicomponent Chemically Reactive Fluid Flow at All Speeds," Los Alamos Scientific Laboratory report LA-8129-MS (1979).
7. Hindmarsh, A. C., "Banded Linear Systems with Pivoting," UCID-30060, Lawrence Livermore Laboratory, Livermore, CA (1970).
8. Larson, R. B., "Numerical Calculations of the Dynamics of a Collapsing Proto-Star," MNRAS, 145, 271 (1969).
9. Hundhausen, A. J. and Gentry, R. A., "Numerical Simulation of Flare-Generated Disturbances in the Solar Wind," J. Geophys. Research, 74, 2908 (1969).
10. Paczynski, B., "Envelopes of Red Supergiants," Acta Astronomica, 19, 1 (1969).
11. Rivard, W. C., Farmer, O. A., Butler, T. D., and O'Rourke, P. J., "A Method for Increased Accuracy in Eulerian Fluid Dynamics Calculations," Los Alamos Scientific Laboratory report LA-5426-MS (1973).

APPENDIX A  
SAMPLE PROBLEM

This appendix provides a listing of SOLA-STAR, a list of main variables, and some information to help the new user convert the code to a non-LASL operating system. We begin by noting that, for the most part, the code is written in ANSI-standard FORTRAN. The CDC computers carry approximately 13 digits, which has proved adequate. However for machines with a short word length, such as IBM, it will be necessary to use double precision throughout the code. This is good practice for any hydrodynamics program, but especially so for SOLA-STAR with its large linear system solver.

SOLA-STAR can be used on quite modest computers. This version of SOLA-STAR requires 77 K<sub>8</sub> words of memory. However, this number can be reduced if necessary by adjusting the size of dimensioned arrays or by sacrificing the plotting capability. The arrays B and AA are dimensioned for a maximum of JBAR = 150 real cells. The grind time, that is the time required to complete one time step for one cell, is 5.3 ms on a CDC 6400. This is approximately a factor of 10 longer than for a CDC 7600 and a factor of 2 larger than for a CDC 6600.

The main system-dependent feature is the graphics package. Logical unit 7 is the film file, and it can be eliminated if graphics output is not desired. The following is a list of graphical output routines used by SOLA-STAR. These routines will have to be replaced by the non-LASL user's local equivalent or deleted from the program.

1. CALL ADV(NF): If  $1 \leq NF \leq 21$ , the film is advanced NF frames. Otherwise, the call is ignored.
2. CALL EMPTY: Empty the FILM file buffer onto disk. Unless the run is unexpectedly aborted, this routine is superfluous.
3. CALL LINCNT(N): N is modulo 64. The next line of output directed to the film file is directed to the Nth line.
4. CALL SPLØT(IOP,N,X,Y,ICHAR,ICØN): Standardized plot routine. Four types of grid: IØP = 1, 2, 3, or 4 gives linear-linear, linear-log, log-linear, or log-log plots respectively. N successive points are plotted from the tables X and Y (abscissas and ordinates respectively). ICHAR is a code number for a character to be plotted at each point

(IC~~ON~~ = 42 is a dot). If IC~~ON~~  $\neq$  0, the points are connected by straight lines.

5. CALL WLCH(IX,IY,CN,NCH,NS): Writes large horizontal characters beginning with SC 4020 coordinates (IX,IY). SC 4020 coordinates define a location on the film frame, with (0,0) at the upper left hand corner and (1023,1023) at the lower right hand corner. NC is the number of characters to be written beginning with the variable NCH. NS is an integer character size parameter,  $1 \leq NS \leq 5$ .

The sample problems in the Appendixes require minor changes to the basic code, and it is convenient to specify the changes in CDC UPDATE format, even though many users will not have this software. A statement of the form \*INSERT SV.n means insert the F~~OR~~TRAN statements between the \*INSERT card and the next statement beginning with an \* behind statement number SV.n. The card \*DELETE SV.m,SV.n means delete statements SV.m through SV.n and replace them with any statements between the \*DELETE and the next \* card. The \*IDENT statement merely specifies a name to be associated with the set of modifications and may be ignored by users not using the UPDATE utility.

Table I lists the major program variables and their definitions. The remainder of this appendix is a program listing and sample output suitable for testing new SOLA-STAR decks. It is recommended that the new user try these problems to become thoroughly familiar with this code before embarking on his or her own research program.

TABLE I

## DEFINITION OF SOLA-STAR VARIABLES

	<u>Definition</u>
AA	Coefficient matrix (band only) of the linear system.
AJ	Areas of cell faces.
B	Right hand side of the linear system.
CND	Thermal conductivity.
D $\phi$ NM	Donor cell parameter $\alpha$ for the $\rho$ and I equations.
D $\phi$ NM $\phi$ M	Donor cell parameter for the u equation.
DT	Time step.
DTK	Maximum allowed value of $ u\delta t/\delta x $ , normally about 0.25.
DTMAX	Maximum value of DT allowed in the run.
DX	Width of the innermost two real cells and left hand fictitious cell.
EI	Specific internal energy I.
EM	Vertex masses.
EMC	Cell masses.
FMASS	Total mass of the system.
FM $\phi$ M	Total momentum of the system.
FOURPI	Four times $\pi$ .
G	Gravitational constant.
GAMMA	$\gamma$ , the ratio of specific heats.
GRDVL	Velocity of grid points as fraction of fluid velocity; zero for Eulerian run, unity for Lagrangian calculation. Can also be fractional or SUBROUTINE GRID can be rewritten to provide an arbitrary, user-chosen grid motion.
JBAR	Number of real cells.
JP1	JBAR + 1.
JP2	JBAR + 2.
JP3	JBAR + 3.
KPR	Get one line summary print every KPR cycles.
LFILM	Get film output every LFILM cycles.
MUVISC	Coefficient of viscosity $\mu$ .

NDIM            Dimension of B and first dimension of AA. Must be at least  
                   NEQ \* JP2.  
 NDIM2           Second dimension of AA.  
 NDT             Number of time steps.  
 NEQ             Number of dependent variables in the linear system.  
 NM              Get full printout every NM cycles.  
 P                Pressure p.  
 PDVCEN         Time centering parameter for  $p\nabla\cdot\vec{u}$  in the I equation.  
 RCV             Reciprocal of the specific heat, T/I.  
 RHØ             Density  $\rho$ .  
 RHOL            Density at the end of Phase I.  
 RMAX            Coordinate r of the right hand boundary.  
 RMIN            Coordinate r of the left hand boundary.  
 RSAV            Central density (RHO(2)) as a function of t. Saved for plotting  
                   purposes only.  
 T                Time t.  
 TIM             Array containing t for use in plotting RSAV.  
 U                Fluid velocity  $u_{j-\frac{1}{2}}$ .  
 UD              Difference velocity  $w_{j-\frac{1}{2}}$ .  
 UG              Grid velocity.  
 UTL             Fluid velocity at the left boundary.  
 UTMAX          Fluid velocity at the right boundary.  
 VJC             Cell volumes.  
 VJV             Vertex volumes.  
 VLAM             $\Lambda$ , the artificial viscosity parameter.  
 UT              Velocity after Phase I.  
 X                Vertex positions  $r_{j-\frac{1}{2}}$ .

PROGRAM VEGA (OUTPUT=100,TAPES=100,TTY,TAPE59=TTY,	SV	2
\$ TAPE5=100)	SV	3
REAL MUVISC	SV	4
COMMON /A1/ JBAR,JP1,JP2,JP3,DT,T,N,NDT,FMASS,FMM,ET,EINT,NM,LFILMSV	SV	5
COMMON /A2/ EM(200),X(200),U(200),MUVISC(200)	SV	6
COMMON /3/ EI(200),E(200),DTMAX,VLAM,DTK	SV	7
COMMON /4/ RHJ(200),EMC(200),P(200),RHJL(200)	SV	8
COMMON /A5/ UT(200),JD(200)	SV	9
COMMON /12/ GAMMA,UT1,UTMAX,DONM,DONMM,GRDVEL	SV	10
COMMON /A14/ EMCT(200),UG(200),DPHI(200)	SV	11
COMMON /A15/ RCV(200),CND(200),R2DR(200),TNOT4	SV	12
COMMON /A40/ FJURPI,AJ(200),XMR(160)	SV	13
COMMON /TIMEV/ R SAV(2000),TIM(2000),ITIME	SV	14
COMMON LA,LB,AA(770,16),JBNEQ,NDIM,IP(770)	SV	15
DIMENSION ZNU(200),THE(200),ALF(200),BET(200),ZKAP(200),TAU(200)	SV	16
DIMENSION B(770),RM(200),RDX(200),AJC(200)	SV	17
DIMENSION RJC(200),VJC(200),RRJC(200),PHI(200),ZJ(200),	SV	18
1 ZN(200),RA(200),RB(200),RC(200),RD(200),VJV(200)	SV	19
DATA T,N/O.,O/	SV	20
DATA FOURPI,G/12.56537062,5.63E-8/	SV	21
DATA PDVCEN/1./	SV	22
DATA LFILM,KPR,NM/25,1,50/	SV	23
C ***	SV	24
C *** SET UP	SV	25
C ***	SV	26
CALL INPUT	SV	27
GM1=GAMMA-1.	SV	28
TNOT4=(EI(JP1)*RCV(JP1))**4	SV	29
WRITE (5,230) TNOT4	SV	30
WRITE (7,230) TNOT4	SV	31
C *** LA IS NUMBER OF ELEMENTS TO LEFT OF DIAGONAL, LB TO RIGHT	SV	32
LA=5	SV	33
LB=5	SV	34
NEQ=5	SV	35
NDIM=770	SV	36
NDIM2=16	SV	37
JBNEQ=JP1+NEQ	SV	38
DO 10 J=2,JP2	SV	39
RDX(J)=1./(X(J+1)-X(J))	SV	40
RJC(J)=.5*(X(J)+X(J+1))	SV	41

	AJC(J)=3.*RJC(J)*RJC(J)	SV	42
	RRJC(J)=0.5/RJC(J)	SV	43
	RA(J)=RDX(J)+2.*RRJC(J)	SV	44
	RB(J)=RDX(J)-2.*RRJC(J)	SV	45
	RC(J)=(RDX(J)+RRJC(J))*RRJC(J)	SV	46
	RD(J)=(RDX(J)-RRJC(J))*RRJC(J)	SV	47
	VJC(J)=X(J+1)**3-X(J)**3	SV	48
	EMC(J)=RHD(J)*VJC(J)	SV	49
10	CONTINUE	SV	50
	RJC(1)=0.5*(X(1)+X(2))	SV	51
C ***	R2DR(2)=0 TO MAKE DI/DR=0 AT ORIGIN	SV	52
	R2DR(2)=0.	SV	53
	DO 20 J=3,JP2	SV	54
	R2DR(J)=1./(X(J+1)-X(J-1))	SV	55
	AJ(J)=3.*X(J)*X(J)	SV	55
	VJV(J)=RJC(J)**3-RJC(J-1)**3	SV	57
20	EM(J)=0.5*(EMC(J-1)+EMC(J))	SV	58
	AJ(2)=3.*X(2)*X(2)	SV	59
	AJ(JP3)=3.*X(JP3)*X(JP3)	SV	60
	VJV(2)=RJC(2)**3-X(2)**3	SV	61
	EM(2)=0.5*EMC(2)	SV	62
	CALL CONDUCT	SV	63
	CALL OUTPUT	SV	64
	DTT=DT	SV	65
	ITIME=0	SV	65
C ***		SV	67
C ***	HYDRDYNAMICS LOOP	SV	68
C ***		SV	69
	DO 200 N=1,NDT	SV	70
	ITIME=ITIME+1	SV	71
	IF (ITIME.GT.500) ITIME=1	SV	72
	DT=AMIN1(DTT,1.1*DT)	SV	73
	T=T+DT	SV	74
	TEMPE=EI(2)*RCV(2)	SV	75
	IF(MOD(N,KPR).EQ.0) WRITE (6,220) DT,T,N,RHD(2),U(15),TEMPE	SV	76
	IF (MOD(N,KPR).EQ.0) WRITE (7,220) DT,T,N,RHD(2),U(15),TEMPE	SV	77
	IF (TEMPE .GT. 3000.) CALL EXIT	SV	78
	JBM=JBAR-1	SV	79
	BET(2)=0.	SV	80
	BET(JP2)=X(JP2)**2*RDX(JP1)	SV	81

DPHI(2)=0.	SV	82
SUM=0.	SV	83
DUG=FJURPI*G/3.	SV	84
DO 30 J=3,JP1	SV	85
SET(J)=X(J)*X(J)/(RJC(J)-RJC(J-1))	SV	86
SUM=SUM+EMC(J-1)*DUG	SV	87
DPHI(J)=SUM/(X(J)*X(J))	SV	88
30 CONTINUE	SV	89
DPHI(JP2)=(SUM+EMC(JP1)*DUG)/(X(JP2)*X(JP2))	SV	90
GMAX=ABS(DPHI(JP2))	SV	91
CALL CONDUCT	SV	92
R2DR(JP3)=0.	SV	93
DO 80 J=2,JP2	SV	94
T1=U(J+1)-U(J)	SV	95
T2=U(J+1)+U(J)	SV	96
T3=0.	SV	97
IF (J.NE.JP2) T3=DT/EMC(J)	SV	98
ZD=T1*RDX(J)+2.*T2*RRJC(J)	SV	99
T4=-DT/(1.+DT*ZD)	SV	100
T5=2.*T1*RDX(J)**2	SV	101
T6=4.*T2*RRJC(J)**2	SV	102
SET(J)=(T1*RDX(J))**2+2.*(T2*RRJC(J))**2	SV	103
ZNU(J)=0.5*T3	SV	104
ALF(J)=2.*T3*MUVISC(J)*VJC(J)	SV	105
THE(J)=U(J+1)*AJ(J+1)-U(J)*AJ(J)	SV	106
ZKAP(J)=T5+T6	SV	107
TAU(J)=T5-T6	SV	108
RM(J)=DT/EM(J)	SV	109
PHI(J)=T4*R4D(J)	SV	110
30 CONTINUE	SV	111
C *** MATRIX STRUCTURE	SV	112
C ***	SV	113
C *** FORMAT BLOCK	SV	114
C ***	SV	115
C	SV	116
C	SV	117
C	SV	118
C	SV	119
C	SV	120
C	SV	121



30

C  
C  
C  
C  
C  
C

```

RHO          K+2,L-2
FLUX          K+3,L+1
EI           K+4,L-1

DO 90 I=1,NDIM
DO 90 J=1,NDIM2
90 AA(I,J)=0.
AA(2,6)=1.
AA(4,7)=1.
K=1-NEQ
L=LA+1
DIVR=0.
ARTPP=0.
DO 120 J=2,JP2
K=K+NEQ
AA(K,L)=-GM1*EI(J)
AA(K,L+2)=1.
AA(K,L+3)=-GM1*RHO(J)
JIVL=DIVR
DIVR=0.
IF (J .LT. JP2) DIVR=(AJ(J+1)*U(J+1)-AJ(J)*U(J))/VJC(J)
IF (DIVR .GT. 0.) DIVR=0.
ARTPM=ARTPP
ARTPP=VLAM*RHO(J)*DIVR/DIVR/(RDX(J)*RDX(J))
IF(J .EQ. 2) GO TO 100
AA(K+1,L-5)=-4.*VJV(J)*RM(J)*MUVISC(J-1)*(R2DR(J)*RDX(J-1)-RC(J-1)
1)
AA(K+1,L-4)=-RM(J)*AJ(J)
AA(K+1,L)=1.+4.*VJV(J)*RM(J)*(MUVISC(J)*(R2DR(J)*RDX(J)+RC(J))
1 +MUVISC(J-1)*(R2DR(J)*RDX(J-1)-RD(J-1)))
AA(K+1,L+1)=RM(J)*AJ(J)
AA(K+1,L+5)=-4.*VJV(J)*RM(J)*MUVISC(J)*(R2DR(J)*RDX(J)+RD(J))
AA(K+3,L-5)=2.*CND(J)*RCV(J)*R2DR(J)
AA(K+3,L+1)=1.
AA(K+3,L)=-2.*CND(J)*RCV(J+1)*R2DR(J)
100 AA(K+4,L-3)=ALF(J)*TAU(J)-PDVCEN*ZNU(J)*P(J)*AJ(J)*2.
AA(K+4,L-2)=2.*ZNU(J)*THE(J)
$ *PDVCEN

```

```

SV 122
SV 123
SV 124
SV 125
SV 126
SV 127
SV 128
SV 129
SV 130
SV 131
SV 132
SV 133
SV 134
SV 135
SV 136
SV 137
SV 138
SV 139
SV 140
SV 141
SV 142
SV 143
SV 144
SV 145
SV 146
SV 147
SV 148
SV 149
SV 150
SV 151
SV 152
SV 153
SV 154
SV 155
SV 156
SV 157
SV 158
SV 159
SV 160
SV 161

```

AA(K+4,L-1)=1.	SV	162
IF (J.EQ.JP2) GO TO 110	SV	163
AA(K+4,L)=2.*ZNU(J)*AJ(J)	SV	164
AA(K+4,L+5)=-2.*ZNU(J)*AJ(J+1)	SV	165
110 CONTINUE	SV	166
AA(K+4,L+2)=2.*PDVCEN*ZNJ(J)*P(J)*AJ(J+1)-ALF(J)*ZKAP(J)	SV	167
AA(K+2,L-2)=1.	SV	168
AA(K+2,L-1)=PHI(J)*RB(J)	SV	169
AA(K+2,L+4)=-PHI(J)*RA(J)	SV	170
B(K)=-3M1*RHO(J)*EI(J)	SV	171
B(K+1)=U(J)	SV	172
IF (J .GT. 2) B(K+1)=B(K+1)+RM(J)*AJ(J)*(ARTPM-ARTPP)	SV	173
B(K+1)=B(K+1)-DT*DPHI(J)	SV	174
B(K+2)=RHO(J)	SV	175
B(K+3)=0.	SV	176
B(K+4)=EI(J)-ALF(J)*BET(J)-DT*ARTPP*DIVR/RHO(J)	SV	177
\$ +2.*(2.*PDVCEN-1.)*ZNU(J)*THE(J)*P(J)	SV	178
120 CONTINUE	SV	179
AA(K+1,L-5)=0.	SV	180
AA(K+1,L-4)=0.	SV	181
AA(K+1,L+1)=0.	SV	182
AA(K+1,L+5)=0.	SV	183
AA(K+1,L)=1.	SV	184
B(K+1)=0.	SV	185
AA(K,L)=0.	SV	186
AA(K,L+3)=0.	SV	187
AA(K,L-3)=-1.	SV	188
B(K)=0.	SV	189
AA(K+2,L-1)=0.	SV	190
AA(K+2,L+4)=0.	SV	191
CALL DECB (IER)	SV	192
CALL SOLB (B)	SV	193
K=1-NEQ	SV	194
GO 130 J=2,JP2	SV	195
K=K+NEQ	SV	196
RHOL(J)=B(K)	SV	197
UT(J)=B(K+1)	SV	198
P(J)=B(K+2)	SV	199
EI(J)=B(K+3)	SV	200
DPHI(J)=B(K+4)	SV	201

32	130	CONTINUE	SV	202
		JT(2)=UT1	SV	203
		RHOL(1)=RHOL(2)	SV	204
		RHOL(JP2)=RHOL(JP1)	SV	205
C	***		SV	206
C	***	REZONE SECTION	SV	207
C	***		SV	208
		CALL GRID	SV	209
		DO 150 J=2,JP1	SV	210
		DUB1=-ABS(DONM)*SIGN(1.,UD(J))	SV	211
		DUB2=-ABS(DONM)*SIGN(1.,UD(J+1))	SV	212
		EMCT(J)=EMC(J)-0.5*DT*(JD(J)*AJ(J)*((1.+DUB1)*RHOL(J-1)+(1.-DUB1)*SV	213	
		1RHOL(J))-JD(J+1)*AJ(J+1)*((1.+DUB2)*RHOL(J)+(1.-DUB2)*RHOL(J+1)))	SV	214
		E(J)=(EI(J)*EMC(J)-.5*DT*(JD(J)*AJ(J)*((1.+DUB1)*RHOL(J-1)*EI(J-1)	SV	215
		1+(1.-DUB1)*RHOL(J)*EI(J))-UD(J+1)*AJ(J+1)*((1.+DUB2)*RHOL(J)*EI(J)	SV	216
		2+(1.-DUB2)*RHOL(J+1)*EI(J+1))))/EMCT(J)	SV	217
	150	CONTINUE	SV	218
		EMCT(JP2)=EMC(JP2)	SV	219
		E(JP2)=EI(JP2)	SV	220
		DO 160 J=3,JP2	SV	221
		DUB1=-ABS(DONM)*SIGN(1.,UD(J)+UD(J-1))	SV	222
		DUB2=-ABS(DONM)*SIGN(1.,UD(J)+UD(J+1))	SV	223
		U(J)=EM(J)*UT(J)-.25*DT*(RHOL(J-1)*(JD(J)+UD(J-1))*AJC(J-1)*((1.+	SV	224
		1DUB1)*UT(J-1)+(1.-DUB1)*JT(J))-RHOL(J)*(UD(J)+UD(J+1))*AJC(J)*	SV	225
		2(1.+DUB2)*UT(J)+(1.-DUB2)*UT(J+1)))	SV	226
	160	CONTINUE	SV	227
		U(JP2)=0.	SV	228
		DPHI(2)=0.	SV	229
		DO 170 J=2,JP2	SV	230
		RDX(J)=1./(X(J+1)-X(J))	SV	231
		RJC(J)=.5*(X(J)+X(J+1))	SV	232
		AJC(J)=3.*RJC(J)*RJC(J)	SV	233
		RRJC(J)=0.5/RJC(J)	SV	234
		RA(J)=RDX(J)+2.*RRJC(J)	SV	235
		RB(J)=RDX(J)-2.*RRJC(J)	SV	236
		RC(J)=(RDX(J)+RRJC(J))*RRJC(J)	SV	237
		RD(J)=(RDX(J)-RRJC(J))*RRJC(J)	SV	238
		VJC(J)=X(J+1)**3-X(J)**3	SV	239
		EMC(J)=EMCT(J)	SV	240
		RHO(J)=EMC(J)/VJC(J)	SV	241

	EI(J)=E(J)	SV	242
170	CONTINUE	SV	243
	RJC(1)=0.5*(X(1)+X(2))	SV	244
	DTT=DTMAX	SV	245
	DO 180 J=3,JP2	SV	246
	R2DR(J)=1./(X(J+1)-X(J-1))	SV	247
	AJ(J)=3.*X(J)*X(J)	SV	248
	VJV(J)=RJC(J)**3-RJC(J-1)**3	SV	249
	EM(J)=0.5*(EMC(J-1)+EMC(J))	SV	250
	U(J)=U(J)/EM(J)	SV	251
	IF (U(J).NE.0.) DTT=AMIN1(DTT,DTK*(X(J+1)-X(J))/ABS(U(J)))	SV	252
180	CONTINUE	SV	253
	VJV(2)=RJC(2)**3-X(2)**3	SV	254
	AJ(2)=3.*X(2)*X(2)	SV	255
	AJ(JP3)=3.*X(JP3)*X(JP3)	SV	256
	EM(2)=0.5*EMCT(2)	SV	257
	U(2)=UT1	SV	258
	RHO(1)=RHO(2)	SV	259
	RHO(JP2)=RHO(JP1)	SV	260
	EI(1)=EI(2)	SV	261
C	***	SV	262
C	*** TIME ACCOUNTING	SV	263
C	***	SV	264
	IF (MOD(N,NM).NE.0 .AND. MOD(N,LFILM).NE.0 .AND. N.GT.1)	SV	265
	\$ GO TO 192	SV	266
	ET=0.	SV	267
	EINT=0.	SV	268
	FMASS=0.	SV	269
	FMOM=0.	SV	270
	DO 190 J=2,JP2	SV	271
	FMOM=FMOM+EM(J)*UT(J)	SV	272
	ET=ET+0.5*EM(J)*UT(J)*UT(J)	SV	273
	IF (J.EQ. JP2) GO TO 190	SV	274
	ET=ET+EMC(J)*EI(J)	SV	275
	EINT=EINT+EMC(J)*EI(J)	SV	276
	FMASS=FMASS+EMC(J)	SV	277
	FMOM=FMOM+EM(J)*UT(J)	SV	278
190	CONTINUE	SV	279
	ET=ET*FOURPI/3.	SV	280
	EINT=EINT*FOURPI/3.	SV	281

	FMASS=FMASS*FOURPI/3.	SV	282
	FMDM=FMDM*FOURPI/3.	SV	283
192	CONTINUE	SV	284
	RSAB(ITIME)=ALOG10(RHO(2))	SV	285
	TIM(ITIME)=T	SV	286
	IF (N.EQ.1) CALL OUTPUT	SV	287
	IF (MJD(N,NM).EQ.0.JR.MJD(N,LFILM).EQ.0) CALL OUTPUT	SV	288
200	CONTINUE	SV	289
	CALL EXIT	SV	290
C ***		SV	291
C ***	FORMAT BLOCK	SV	292
C ***		SV	293
220	FORMAT (2X,4HDT =,1PE17.8,2X,3HT =,E17.8,I5,3E13.5)	SV	294
230	FORMAT (1X,1PE20.8)	SV	295
	END	SV	296
	SUBROUTINE INPUT	SV	297
	COMMON /A1/ JBAR,JP1,JP2,JP3,DT,T,N,NDT,FMASS,FMDM,ET,EINT,NM,LFILMSV	SV	299
	COMMON /A2/ EM(200),X(200),U(200),MUVISC(200)	SV	299
	COMMON /3/ EI(200),E(200),DTMAX,VLAM,DTK	SV	300
	COMMON /4/ RHO(200),EMC(200),P(200),RHOL(200)	SV	301
	COMMON /A5/ UT(200),UD(200)	SV	302
	COMMON /10/ ITITLE(8)	SV	303
	COMMON /12/ GAMMA,UT1,UTMAX,DONM,DONMOM,GRDVEL	SV	304
	COMMON /A14/ EMCT(200),UG(200),DPHI(200)	SV	305
	COMMON /A15/ RCV(200),CND(200),R2DR(200),TNDT4	SV	306
	REAL MUVISC	SV	307
	DATA (EM(J),J=1,200)/200*0./	SV	308
	DATA (MUVISC(J),J=1,200)/200*0./	SV	309
	DATA (UT(J),J=1,200)/200*0./	SV	310
	DATA (U(J),J=1,200)/200*0./	SV	311
	DATA (UG(J),J=1,200)/200*0./	SV	312
	DATA (RCV(J),J=1,200)/200*1.911098562E-08/	SV	313
C ***		SV	314
C ***	READ DATA DECK	SV	315
C ***		SV	316
	READ (5,50) (ITITLE(J),J=1,8)	SV	317
	WRITE (6,50) (ITITLE(J),J=1,8)	SV	318
	WRITE (7,50) (ITITLE(J),J=1,8)	SV	319
	READ (5,60) JBAR,NDT	SV	320
	WRITE (6,60) JBAR,NDT	SV	321

	WRITE (7,60) JBAR,NDT	SV	322
	JP1=JBAR+1	SV	323
	JP2=JP1+1	SV	324
	JP3=JP2+1	SV	325
	READ (5,70) DT,DX,GRDVEL	SV	326
	WRITE (6,70) DT,DX,GRDVEL	SV	327
	WRITE (7,70) DT,DX,GRDVEL	SV	328
	READ (5,70) RMIN,RMAX	SV	329
	WRITE (6,70) RMIN,RMAX	SV	330
	WRITE (7,70) RMIN,RMAX	SV	331
	READ (5,70) DJNM,DONMOM	SV	332
	WRITE (6,70) DONM,DJNMOM	SV	333
	WRITE (7,70) DJNM,DONMOM	SV	334
	READ (5,70) GAMMA,UT1,UTMAX	SV	335
	WRITE (6,70) GAMMA,UT1,UTMAX	SV	336
	WRITE (7,70) GAMMA,UT1,UTMAX	SV	337
	READ (5,70) VLAM,DTMAX,DTK	SV	338
	WRITE (6,70) VLAM,DTMAX,DTK	SV	339
	WRITE (7,70) VLAM,DTMAX,DTK	SV	340
	U(2)=UT1	SV	341
	U(JP2)=UTMAX	SV	342
C	***	SV	343
C	*** SET UP MESH	SV	344
C	***	SV	345
	X(2)=RMIN	SV	346
	RMLD=0.5	SV	347
	RMHI=2.	SV	348
	RATIO=1.	SV	349
	DRB=DX	SV	350
10	CONTINUE	SV	351
	DX=DRB	SV	352
	DO 20 J=3,JP3	SV	353
	IF (J.GT.4.AND.J.LT.JBAR) DX=DX*RATIO	SV	354
	X(J)=X(J-1)+DX	SV	355
20	CONTINUE	SV	356
	WRITE (6,80) RATIO,X(JP2),DX	SV	357
	IF (RATIO.GT.2.95.AND.X(JP2).LT.RMAX) CALL EXIT	SV	358
	IF (ABS((X(JP2)-RMAX)/RMAX).LT.1.E-4) GO TO 30	SV	359
	IF (X(JP2).GT.RMAX) RMHI=RATIO	SV	360
	IF (X(JP2).LE.RMAX) RMLD=RATIO	SV	361

	RATIO=0.5*(RMLD+RMHI)	SV	362
	GO TO 10	SV	363
30	CONTINUE	SV	364
	X(1)=2.*X(2)-X(3)	SV	365
C	***	SV	366
C	*** INITIALIZE DEPENDENT VARIABLES	SV	367
C	***	SV	368
	DO 40 J=1,JP2	SV	369
	RHO(J)=1.10E-19	SV	370
	RHO(J)=1.26E-19	SV	371
	P(J)=3.696E-11	SV	372
	P(J)=4.39758E-11	SV	373
	U(J)=0.	SV	374
	EI(J)=P(J)/((GAMMA-1.)*RHO(J))	SV	375
40	CONTINUE	SV	376
	J(2)=UT1	SV	377
	U(JP3)=U(JP2)	SV	378
	UD(JP3)=0.	SV	379
	UT(JP3)=0.	SV	380
	CALL SETKAP	SV	381
	RETURN	SV	382
C		SV	383
	50 FORMAT (BA10)	SV	384
	60 FORMAT (10H ,I10,10H ,I10)	SV	385
	70 FORMAT (10H ,E10.3,10H ,E10.3,10H ,	SV	386
	1 E10.3)	SV	387
	80 FORMAT (1X,*RATIO, RMAX FROM MESH GEN*,1P3E16.8)	SV	388
	END	SV	389
	SUBROUTINE SETKAP	SV	390
	COMMON/KAPA/KAP(51,31),XMF,YMF,ZMF	SV	391
	REAL KAP	SV	392
C	***	SV	393
C	*** READS GOB OPACITY DECK	SV	394
C	***	SV	395
	READ (5,100) XMF,YMF	SV	396
100	FORMAT (10F8.5)	SV	397
	ZMF=1.-XMF-YMF	SV	398
	I=0	SV	399
	K2=0	SV	400
300	CONTINUE	SV	401

	I=I+1	SV	402
	IF (I .GT. 51) GO TO 304	SV	403
301	FORMAT (1X,I5,14F5.2)	SV	404
	K2=K2+1	SV	405
	READ (5,301) K1,(KAP(I,J),J=1,14)	SV	406
	IF (K1 .NE. K2) GO TO 302	SV	407
	K2=K2+1	SV	408
	READ (5,301) K1,(KAP(I,J),J=15,28)	SV	409
	IF (K1 .NE. <2) GO TO 302	SV	410
	<2=<2+1	SV	411
	READ (5,301) K1,(KAP(I,J),J=29,31)	SV	412
	IF (K1 .NE. K2) GO TO 302	SV	413
	GO TO 300	SV	414
302	CONTINUE	SV	415
303	FORMAT (1X,21HWRONG CAPACITY CARD,K=I3)	SV	416
	WRITE (6,303) K2	SV	417
	CALL EXIT	SV	418
304	CONTINUE	SV	419
	RETURN	SV	420
	END	SV	421
	SUBROUTINE OUTPUT	SV	422
	REAL MUVISC	SV	423
	COMMON /A1/ JBAR, JP1, JP2, JP3, DT, T, N, NDT, FMASS, FMOM, ET, EINT, NM, LFILMSV	SV	424
	COMMON /A2/ EM(200), X(200), U(200), MUVISC(200)	SV	425
	COMMON /A3/ EI(200), E(200), DTMAX, VLAM, DTK	SV	426
	COMMON /A4/ RHO(200), EMC(200), P(200), RHOL(200)	SV	427
	COMMON /A5/ UT(200), UD(200)	SV	428
	COMMON /A6/ ITITLE(8)	SV	429
	COMMON /A7/ GAMMA, JT1, UTMAX, JDNM, DONMOM, GRDVEL	SV	430
	COMMON /A8/ EMCT(200), JG(200), DPHI(200)	SV	431
	COMMON /A9/ RCV(200), CND(200), R2DR(200), TNOT4	SV	432
	COMMON /A10/ FJURPI, AJ(200), XMR(160)	SV	433
	COMMON /TIMEV/ RSAV(2000), TIM(2000), ITIME	SV	434
	DIMENSION AL(200), BL(200), CL(200)	SV	435
	DIMENSION XC(200), TEM(200)	SV	436
	DATA UTITLE/10HX-VELJCITY/	SV	437
	DATA (DPHI(J), J=1, 200)/200*0./	SV	438
	DATA PTITLE/8HPRESSURE/	SV	439
	DATA (XMR(J), J=1, 160)/160*0./	SV	440
	DATA RHDTITL/7HDENSITY/	SV	441
	DATA XITLE/3HSIE/	SV	442



C ***		SV	443
C ***	BCD OUTPUT,	SV	444
C ***		SV	445
	DD 25 J=2,JP2	SV	446
	IF (J .GT. 2) XMR(J)=XMR(J-1)+FOURPI*EMC(J-1)/3.	SV	447
	DPHI(J)=-FOURPI*AJ(J)*DPHI(J)/3.	SV	448
	TEM(J)=EI(J)*RCV(J)	SV	449
25	CONTINUE	SV	450
	IUMIN=6	SV	451
	IUMAX=7	SV	452
	IF (N.LE.1) GO TO 10	SV	453
	IF (MOD(N,NM).NE.0) IUMIN=7	SV	454
	IF (MOD(N,LFILM).NE.0) IUMAX=6	SV	455
	IF (IUMIN.GT.IUMAX) IUMAX=7	SV	456
10	DO 20 IU=IUMIN,IUMAX	SV	457
	WRITE (IU,40) EINT,ET,FMASS,FMDM,N	SV	458
	IF (IU.EQ.7) CALL ADV (1)	SV	459
	WRITE (IU,50)	SV	460
	WRITE (IU,60)(I,X(I),U(I),RHO(I),EI(I),P(I),CND(I),DPHI(I),	SV	461
	1 XMR(I),TEM(I),I=2,JP2)	SV	462
20	CONTINUE	SV	463
C ***		SV	464
C ***	GRAPHICAL OUTPUT	SV	465
C ***		SV	466
	IF (IUMAX .EQ. 6) RETURN	SV	467
	CALL SPLDT (1,JP1,X(2),U(2),42,1)	SV	468
	CALL WLCH (0,0,56,ITITLE,2)	SV	469
	CALL WLCH (0,25,10,UTITLE,1)	SV	470
	CALL LINCNT (60)	SV	471
	WRITE (7,70)T,N	SV	472
	DO 30 J=2,JP1	SV	473
	XC(J)=.5*(X(J)+X(J+1))	SV	474
	AL(J)=ALOG10(RHO(J))	SV	475
	BL(J)=ALOG10(EI(J))	SV	476
	CL(J)=ALOG10(P(J))	SV	477
30	CONTINUE	SV	478
	CALL SPLDT (1,JP1-1,XC(2),P(2),42,1)	SV	479
	CALL WLCH (0,0,56,ITITLE,2)	SV	480
	CALL WLCH (0,25,8,PTITLE,1)	SV	481
	CALL LINCNT (60)	SV	482

WRITE (7,70)T,N	SV	483
CALL SPLOT (1,JP1-1,XC(2),EI(2),42,1)	SV	484
CALL WLCH (0,0,55,ITITLE,2)	SV	485
CALL WLCH (0,25,3,XITILE,1)	SV	486
CALL LINCNT (60)	SV	487
WRITE (7,70)T,N	SV	488
CALL SPLOT (1,JP1-1,XC(2),RHD(2),42,1)	SV	489
CALL WLCH (0,0,56,ITITLE,2)	SV	490
CALL WLCH (0,25,7,RHOTITL,1)	SV	491
CALL LINCNT (60)	SV	492
WRITE (7,70)T,N	SV	493
CALL SPLOT (1,JP1-1,XC(2),CND(2),42,1)	SV	494
CALL WLCH (0,0,55,ITITLE,2)	SV	495
CALL WLCH (0,25,3,3HCND,1)	SV	496
CALL LINCNT (50)	SV	497
WRITE (7,70)T,N	SV	498
IF (N.GT.10) CALL SPLOT (2,ITIME,TIM,RSAB,42,1)	SV	499
IF (N.GT.10) CALL WLCH (0,25,8,8HRHD VS T,1)	SV	500
CALL LINCNT (60)	SV	501
WRITE (7,70)T,N	SV	502
JBAR=JP1-1	SV	503
CALL SPLOT (2,JBAR,XC(2),AL(2),42,1)	SV	504
CALL WLCH(0,25,7,RHOTITL,1)	SV	505
CALL SPLOT (2,JBAR,XC(2),BL(2),42,1)	SV	506
CALL WLCH(0,25,3, XITILE,1)	SV	507
CALL SPLOT (2,JBAR,XC(2),CL(2),42,1)	SV	508
CALL WLCH(0,25,8,PTITLE,1)	SV	509
XJCL=1.E-3*X(JP2)	SV	510
DO 7000 J=2,JP1	SV	511
JCL=J	SV	512
IF (X(J) .GT. XJCL) GO TO 7001	SV	513
7000 CONTINUE	SV	514
7001 CONTINUE	SV	515
IF (JCL .EQ. JP1 .OR. JCL .LT. 3) GO TO 7002	SV	516
CALL SPLOT(1,JCL,X(2),U(2),42,1)	SV	517
CALL WLCH(0,25,10,UTITLE,1)	SV	518
CALL SPLOT(1,JCL-1,XC(2), P(2),42,1)	SV	519
CALL WLCH(0,25,8,PTITLE,1)	SV	520
CALL SPLOT(1,JCL-1,XC(2), EI(2),42,1)	SV	521
CALL WLCH(0,25,3, XITILE,1)	SV	522

	CALL SPLOT(1,JCL-1,XC(2),RHO(2),42,1)	SV	523
	CALL #LC+(0,25,7,RHOTITL,1)	SV	524
7032	CONTINUE	SV	525
	WRITE (59,70) T,N	SV	526
	IF (TEM(2) .GT. 2000.) CALL EXIT	SV	527
	RETURN	SV	528
C	***	SV	529
C	*** FORMAT BLOCK	SV	530
C	***	SV	531
	40 FORMAT (1X,17HINTERNAL ENERGY =,1PE13.6,	SV	532
	1 15H TOTAL ENERGY =,E13.6,7H MASS =,E13.6,11H MOMENTUM =,E13.6,	SV	533
	1 8H CYCLE =,I7)	SV	534
	50 FORMAT (4X,1HJ,7X,1HX,12X,1HU,11X,3HR40,10X,2HEI,11X,1HP,	SV	535
	\$ 10X,3HCND,11X,1HL,10X,24MR,11X,1HT)	SV	536
	60 FORMAT (1X,I3,1P9E13.5)	SV	537
	70 FORMAT (5H TIME =,1PE10.3,7H CYCLE =,I5)	SV	538
	END	SV	539
	SUBROUTINE GRID	SV	540
	REAL MUVISC	SV	541
	COMMON /A1/ JBAR,JP1,JP2,JP3,DT,T,N,NDT,FMASS,FMOM,ET,EINT,NM,LFILMSV	SV	542
	COMMON /A2/ EM(200),X(200),U(200),MUVISC(200)	SV	543
	COMMON /A5/ UT(200),JD(200)	SV	544
	COMMON /I2/ GAMMA,UT1,UTMAX,DONM,DONMOM,GRDVEL	SV	545
	COMMON /A14/ EMCT(200),UG(200),DPHI(200)	SV	546
C	***	SV	547
C	*** DEFINE GRID VELOCITY UG, REZONE (DIFFERENCE) VELOCITY UD,	SV	548
C	*** AND NEW VERTEX POSITIONS X.	SV	549
C	*** GRDVEL = 0., EULERIAN. GRDVEL = 1., LAGRANGIAN.	SV	550
C	***	SV	551
	DO 10 J=2,JP2	SV	552
	JG(J)=GRDVEL*UT(J)	SV	553
	UD(J)=UG(J)-UT(J)	SV	554
	X(J)=X(J)+DT*UG(J)	SV	555
	10 CONTINUE	SV	556
	X(JP3)=2.*X(JP2)-X(JP1)	SV	557
	X(1)=2.*X(2)-X(3)	SV	558
	RETURN	SV	559
	END	SV	560
	REAL FUNCTION KAPPA(RD1,TE)	SV	561
C	*** T LIMITS OF TABLE ARE LOG(T)=3.3 AND 3.2	SV	562

C ***	RHO TABLE LIMITS ARE 1.E-12 AND 1000.	SV	563
	COMMON/KAPA/KAP(51,31),XMF,YMF,ZMF	SV	564
	REAL KAP,KAPP	SV	565
	INTEGER DI,TI	SV	566
	DATA DUSTK/0.15/	SV	567
C ***	DUST OPACITY ONLY	SV	568
	KAPPA=DUSTK	SV	569
	IF (TE .LE. 1500.) RETURN	SV	570
C ***	GAS OPACITY	SV	571
	RD=RD1	SV	572
	D=2.0*ALOG10(RD)+25.0	SV	573
	DI=INT(D)	SV	574
	D=D-DI	SV	575
	T=20.*ALOG10(TE)-65.	SV	576
	IF (T .GT. 35.) T=35.+(T-35.)*0.25	SV	577
	TI=INT(T)	SV	578
	T=T-TI	SV	579
	IF (DI .GE. 1) GO TO 30	SV	580
	DI=1	SV	581
	D=0.	SV	582
30	CONTINUE	SV	583
	IF (DI .LE. 30) GO TO 31	SV	584
	DI=30	SV	585
	D=1.	SV	586
31	CONTINUE	SV	587
	IF (TI .GE. 1) GO TO 32	SV	588
	TI=1	SV	589
	T=0.	SV	590
32	CONTINUE	SV	591
	IF (TI .LE. 50) GO TO 33	SV	592
	TI=50	SV	593
	T=1.	SV	594
33	$KAPP=(1.-T)*((1.-D)*KAP(TI,DI)+D*KAP(TI,DI+1))+$	SV	595
1	$T*((1.-D)*KAP(TI+1,DI)+D*KAP(TI+1,DI+1))$	SV	596
	KAPPA=EXP(2.3026*KAPP)	SV	597
	IF (TE .GE. 2000.) RETURN	SV	598
C ***	DUST PLUS GAS OPACITIES	SV	599
	T=(2000.-TE)*0.002	SV	600
	KAPPA=T*DUSTK+(1.-T)*KAPPA	SV	601
	RETURN	SV	602

	END	SV	603
	SUBROUTINE CONDUCT	SV	604
	REAL KAPPA, MUVISC	SV	605
	COMMON /A1/ JBAR, JP1, JP2, JP3, DT, T, N, NDT, FMASS, FMOM, ET, EINT, NM, LFILMSV	SV	606
	COMMON /A2/ E4(200), X(200), U(200), MUVISC(200)	SV	607
	COMMON /3/ EI(200), E(200), DTMAX, VLAM, DTK	SV	608
	COMMON /4/ RHO(200)	SV	609
	COMMON /A15/ RCV(200), CND(200), R2DR(200), TNOT4	SV	610
	DATA PR/1.0/	SV	611
C	***	SV	612
C	*** COMPUTE CONDUCTIVITY CND AND VISCOSITY MUVISC.	SV	613
C	***	SV	614
	DD 10 J=2, JP1	SV	615
	TEM=EI(J)*RCV(J)	SV	616
	MUVISC(J)=7.15E-05*SQRT(TEM)	SV	617
	TEM=0.5*(TEM+EI(J-1)*RCV(J-1))	SV	618
	RDE=0.5*(RHO(J)+RHO(J-1))	SV	619
	AA=RDE*TEM*KAPPA(RDE, TEM)	SV	620
	TGRAD=2.*(RCV(J)*EI(J)-EI(J-1)*RCV(J-1))*R2DR(J)	SV	621
	CND(J)=3.02383E-04*(TEM**4-TNOT4)/((1.-4.*TGRAD/(3.*AA))*AA)	SV	622
C	CND(J)=3.02383E-04*TEM*TEM*TEM/(RDE*KAPPA(RDE, TEM))	SV	623
C	CND(J)=0.5*(MUVISC(J)+MUVISC(J-1))/PR	SV	624
	10 CONTINUE	SV	625
	MUVISC(1)=MUVISC(2)	SV	626
	MUVISC(JP2)=MUVISC(JP1)	SV	627
	CND(JP1)=CND(JP1-1)	SV	628
	CND(JP1+1)=CND(JP1)	SV	629
	RETURN	SV	630
	END	SV	631
	SUBROUTINE DECB(IER)	SV	632
	COMMON ML, MU, B(770,15), N, NDIM, IP(770)	SV	633
C		SV	634
C	LU DECOMPOSITION OF BAND MATRIX A.. L*U=P*A, WHERE P IS A	SV	635
C	PERMUTATION MATRIX, L IS A UNIT LOWER TRIANGULAR MATRIX,	SV	636
C	AND U IS AN UPPER TRIANGULAR MATRIX.	SV	637
C	N = CRDER OF MATRIX.	SV	638
C	B = N BY (2*ML+MU+1) ARRAY CONTAINING THE MATRIX A ON INPUT	SV	639
C	AND ITS FACTORED FORM ON OUTPUT.	SV	640
C	ON INPUT, B(I,K) (1.LE.I.LE.N) CONTAINS THE K-TH	SV	641
C	DIAGONAL OF A, OR A(I,J) IS STORED IN B(I,J-I+ML+1).	SV	642

C	ON OUTPUT, B CONTAINS THE L AND U FACTORS, WITH	SV	643
C	U IN COLUMNS 1 TO ML+MU+1, AND L IN COLUMNS	SV	644
C	ML+MU+2 TO 2*ML+MU+1.	SV	645
C	ML,MU= WIDTHS OF THE LOWER AND UPPER PARTS OF THE BAND, NOT	SV	646
C	COUNTING THE MAIN DIAGONAL. TOTAL BANDWIDTH IS ML+MU+1.	SV	647
C	NDIM = THE FIRST DIMENSION (COLUMN LENGTH) OF THE ARRAY B.	SV	648
C	NDIM MUST BE . GE. N.	SV	649
C	IP = ARRAY OF LENGTH N CONTAINING PIVOT INFORMATION.	SV	650
C	IER = ERROR INDICATOR..	SV	651
C	= 0 IF NO ERROR,	SV	652
C	= K IF THE K-TH PIVOT CHOSEN WAS ZERO ( A IS SINGULAR).	SV	653
C	CAUTION.. IF ML=0, THIS ROUTINE CONTAINS EMPTY DO-LOOPS	SV	654
C	WHICH MUST BE COMPILED CORRECTLY (I.E.NO ACTION TAKEN).	SV	655
C	THE INPUT ARGUMENTS ARE NDIM,N,ML,MU,B.	SV	656
C	THE OUTPUT ARGUMENTS ARE B,IP,IER.	SV	657
C		SV	658
	IER=0	SV	659
	LL=ML+MU+1	SV	660
	N1=N-1	SV	661
	DO 3 I=1,ML	SV	662
	II=MU+I	SV	663
	K=ML+1-I	SV	664
	DO 1 J=1,II	SV	665
1	B(I,J)=B(I,J+K)	SV	666
	K=II+1	SV	667
	DO 2 J=K,LL	SV	668
2	B(I,J)=0.	SV	669
3	CONTINUE	SV	670
	LR=ML	SV	671
	DO 9 NR=1,N1	SV	672
	NP=NR+1	SV	673
	IF( LR.NE.N) LR=LR+1	SV	674
	MX=NR	SV	675
	XM=ABS(B(NR))	SV	676
	DO 4 I=NP,LR	SV	677
	IF(ABS(B(I)).LE.XM)GO TO 4	SV	678
	MX=I	SV	679
	XM=ABS(B(I))	SV	680
4	CONTINUE	SV	681
	IP(NR)=MX	SV	682

	IF(MX.EQ.NR)GO TO 6	SV	683
	DO 5 I=1,LL	SV	684
	XX=B(NR,I)	SV	685
	B(NR,I)=B(MX,I)	SV	686
5	B(MX,I)=XX	SV	687
6	XM=B(NR)	SV	688
	IF(XM.EQ.0.)GO TO 10	SV	689
	B(NR)=1./XM	SV	690
	XM=-B(NR)	SV	691
	KK=MIND(N-NR,LL-1)	SV	692
	DO 8 I=NP,LR	SV	693
	J=LL+I-NR	SV	694
	XX=B(I)*XM	SV	695
	B(NR,J)=XX	SV	696
	DO 7 II=1,KK	SV	697
7	B(I,II)=B(I,II+1)+XX*B(NR,II+1)	SV	698
8	B(I,LL)=0.	SV	699
9	CONTINUE	SV	700
	NR=N	SV	701
	IF(B(N).EQ.0.)GO TO 10	SV	702
	B(N)=1./B(N)	SV	703
	RETURN	SV	704
10	IER=NR	SV	705
	RETURN	SV	706
	END	SV	707
	SUBROUTINE SOLB(Y)	SV	708
	COMMON ML,MU,B(770,16),N,NDIM,IP(770)	SV	709
	DIMENSION Y(1)	SV	710
C		SV	711
C	SOLUTION OF A*X=C GIVEN LU DECOMPOSITION OF A FROM DECB.	SV	712
C	Y = RIGHT-HAND VECTOR C, OF LENGTH N, ON INPUT,	SV	713
C	= SOLUTION VECTOR X ON OUTPUT.	SV	714
C	CAUTION.. IF ML=0, THIS ROUTINE CONTAINS EMPTY DO-LOOPS	SV	715
C	WHICH MUST BE COMPILED CORRECTLY (I.E. NO ACTION TAKEN).	SV	716
C	ALL THE ARGUMENTS ARE INPUT ARGUMENTS.	SV	717
C	THE OUTPUT ARGUMENT IS Y.	SV	718
C		SV	719
	N1=N-1	SV	720
	LL=ML+MU+1	SV	721
	DO 3 NR=1,N1	SV	722

	IF(IP(NR).EQ.NR)GO TO 1	SV	723
	J=IP(NR)	SV	724
	XX=Y(NR)	SV	725
	Y(NR)=Y(J)	SV	726
	Y(J)=XX	SV	727
1	KK=MINO(N-NR,ML)	SV	728
	DO 2 I=1,KK	SV	729
2	Y(NR+I)=Y(NR+I)+Y(NR)*B(NR,LL+I)	SV	730
3	CONTINUE	SV	731
	LL=LL-1	SV	732
	Y(N)=Y(N)*B(N)	SV	733
	KK=0	SV	734
	DO 5 NB=1,N1	SV	735
	NR=N-N3	SV	736
	IF(KK.NE.LL)KK=KK+1	SV	737
	DP=0.	SV	738
	DO 4 I=1,KK	SV	739
4	DP=DP+B(NR,I+1)*Y(NR+I)	SV	740
5	Y(NR)=(Y(NR)-DP)*3(NR)	SV	741
	RETURN	SV	742
	END	SV	743
	SUBROUTINE UNDRP	SV	744
	CALL GFR80(1HU,4HVEGA,4,3H105,5HT3LDC,4HKEEP)	SV	745
	CALL GRPHLUN(7)	SV	746
	CALL LIB4020	SV	747
	CALL GRPHFTN	SV	748
	CALL SETFLSH	SV	749
	RETURN	SV	750
	END	SV	751



```
***** *IDENT FIX
***** *DELETE SV.23
          DATA LFIL4,KPR,NM/130,5,500/
***** *INSERT SV.371
          IF (J.LE.5) RHO(J)=RHO(J)+FLOAT(10-MAXO(2,J))*0.25
***** *INSERT SV.26
          CALL UNDRP
```

```

1 10/26/77 EXPJRT VEGA BASE CASE
2 JBAR          120   NDT          4000
3 DT           1.000E+010DX       3.000E+012 GRDVEL       0.0
4 RMIN         0.000E+000 RMAX     1.560E+017
5 DGNR MASS    1.0   DGNR MOM     1.0
6 GAMMA        1.657UT1          UTMAX
7 VLAM         0.   DTMAX       +1.000E+10 DTK          0.20
8   .70000   .27000
9   1-4.45-3.30-3.20-2.85-2.72-2.67-2.64-2.63-2.53-2.62-2.62-2.62-2.61-2.60
10  2-2.50-2.59-2.58-2.55-2.54-2.52-2.49-2.46-2.42-5.54-4.59-4.59-4.59-4.59
11  3-4.59-4.59-4.59
12  4-4.73-4.71-4.59-4.14-3.52-3.04-2.80-2.69-2.65-2.53-2.51-2.60-2.59-2.57
13  5-2.55-2.52-2.49-2.44-2.39-2.33-2.26-2.18-2.09-5.32-4.41-4.41-4.41-4.41
14  6-4.41-4.41-4.41
15  7-4.53-4.51-4.43-4.41-4.29-4.05-3.50-3.12-2.83-2.69-2.62-2.57-2.53-2.48
16  8-2.43-2.36-2.29-2.20-2.09-1.98-1.85-1.72-1.58-5.09-4.23-4.23-4.23-4.23
17  9-4.23-4.23-4.23
18 10-4.44-4.41-4.38-4.31-4.21-4.08-3.90-3.54-3.28-2.90-2.60-2.41-2.25-2.13
19 11-2.01-1.88-1.73-1.59-1.43-1.28-1.12 -.95 -.80-4.67-4.05-4.05-4.05-4.05
20 12-4.05-4.05-4.05
21 13-4.31-4.29-4.32-4.24-4.10-3.92-3.68-3.39-3.06-2.72-2.38-2.07-1.92-1.62
22 14-1.45-1.27-1.08 -.90 -.71 -.52 -.33 -.14 .00-4.55-3.87-3.87-3.87-3.87
23 15-3.87-3.87-3.87
24 16-4.13-4.14-4.23-4.12-3.94-3.58-3.37-3.04-2.69-2.35-2.03-1.72-1.44-1.20
25 17 -.93 -.75 -.53 -.30 -.08 .15 .38 .51 .66-4.43-3.70-3.70-3.70-3.70
26 18-3.70-3.70-3.70
27 19-3.95-3.99-4.03-3.92-3.71-3.39-3.03-2.59-2.35-2.04-1.73-1.43-1.13 -.86
28 20 -.60 -.35 -.06 .21 .47 .74 1.01 1.25 1.06-4.21-3.52-3.52-3.52-3.52
29 21-3.52-3.52-3.52
30 22-3.41-3.40-3.56-3.52-3.37-3.12-2.82-2.51-2.17-1.82-1.47-1.13 -.80 -.51
31 23 -.24 .00 .35 .61 .89 1.17 1.46 1.72 1.25-3.99-3.34-3.34-3.34-3.34
32 24-3.34-3.34-3.34
33 25-2.63-2.79-2.95-2.98-2.93-2.78-2.55-2.28-1.96-1.59-1.21 -.84 -.50 -.20
34 26 .03 .37 .66 .95 1.25 1.54 1.83 2.03 1.39-3.77-3.16-3.16-3.16-3.16
35 27-3.16-3.16-3.16
36 28-1.90-2.05-2.24-2.37-2.39-2.27-2.06-1.81-1.53-1.23 -.91 -.58 -.26 .05
37 29 .36 .57 .98 1.29 1.60 1.91 2.22 2.45 1.51-3.55-2.98-2.98-2.98-2.98
38 30-2.98-2.98-2.98
39 31-1.27-1.39-1.49-1.51-1.66-1.56-1.39-1.18 -.96 -.72 -.47 -.20 .09 .38
40 32 .53 .97 1.23 1.58 1.88 2.18 2.47 2.66 1.61-3.33-2.80-2.80-2.80-2.80

```



81	73	-.47	-.47	-.47	-.42	-.32	-.18	.03	.38	.32	1.33	1.88	2.42	2.95	3.46
82	74	3.95	4.40	4.79	5.11	5.35	5.41	5.08	4.27	3.03	-.24	-.29	-.29	-.29	-.29
83	75	-.29	-.29	-.29											
84	76	-.47	-.47	-.47	-.44	-.36	-.23	-.02	.32	.75	1.25	1.80	2.33	2.85	3.38
85	77	3.83	4.34	4.76	5.10	5.34	5.39	5.09	4.33	3.12	-.01	-.11	-.11	-.11	-.11
86	78	-.11	-.11	-.11											
87	79	-.47	-.47	-.47	-.45	-.40	-.28	-.07	.26	.68	1.18	1.72	2.24	2.76	3.28
88	80	3.73	4.25	4.68	5.05	5.30	5.32	5.07	4.38	3.22	.21	.07	.07	.07	.07
89	81	.07	.07	.07											
90	82	-.47	-.47	-.47	-.47	-.44	-.32	-.12	.20	.60	1.10	1.63	2.14	2.65	3.16
91	83	3.67	4.15	4.53	4.95	5.20	5.22	5.00	4.42	3.32	.43	.25	.25	.25	.25
92	84	.25	.25	.25											
93	85	-.47	-.47	-.47	-.49	-.47	-.36	-.16	.14	.52	1.00	1.52	2.02	2.52	3.04
94	86	3.54	4.01	4.44	4.82	5.07	5.05	4.88	4.43	3.41	.65	.43	.43	.43	.43
95	87	.43	.43	.43											
96	88	-.47	-.47	-.47	-.49	-.48	-.39	-.23	.01	.35	.80	1.31	1.82	2.34	2.87
97	89	3.39	3.87	4.30	4.67	4.92	4.93	4.81	4.45	3.51	.87	.61	.61	.61	.61
98	90	.61	.61	.61											
99	91	-.47	-.47	-.47	-.49	-.48	-.42	-.30	-.11	.17	.60	1.10	1.61	2.15	2.70
100	92	3.22	3.71	4.14	4.50	4.76	4.80	4.73	4.45	3.60	1.09	.79	.79	.79	.79
101	93	.79	.79	.79											
102	94	-.47	-.47	-.47	-.48	-.47	-.44	-.36	-.22	.01	.39	.87	1.39	1.94	2.50
103	95	3.04	3.54	3.97	4.34	4.59	4.68	4.65	4.47	3.69	1.31	.97	.97	.97	.97
104	96	.97	.97	.97											
105	97	-.47	-.47	-.47	-.48	-.47	-.45	-.41	-.30	-.09	.25	.68	1.13	1.72	2.29
106	98	2.85	3.36	3.81	4.19	4.47	4.53	4.59	4.44	3.77	1.53	1.15	1.15	1.15	1.15
107	99	1.15	1.15	1.15											
108	100	-.47	-.47	-.47	-.47	-.47	-.47	-.44	-.35	-.17	.12	.51	.98	1.50	2.07
109	101	2.64	3.17	3.65	4.05	4.35	4.49	4.52	4.39	3.82	1.75	1.32	1.32	1.32	1.32
110	102	1.32	1.32	1.32											
111	103	-.47	-.47	-.47	-.47	-.47	-.49	-.47	-.39	-.23	.01	.34	.73	1.29	1.85
112	104	2.43	2.98	3.48	3.91	4.23	-.39	4.43	4.30	3.84	1.97	1.50	1.20	.71	-.27
113	105	-1.20	-2.29	-3.39											
114	106	-.47	-.47	-.47	-.47	-.47	-.48	-.49	-.46	-.40	-.30	-.13	.15	.55	1.07
115	107	1.63	2.22	2.76	3.21	3.54	3.74	3.82	3.79	3.65	2.79	2.20	1.75	1.19	.24
116	108	-.70	-1.77	-2.86											
117	109	-.47	-.47	-.47	-.47	-.47	-.47	-.47	-.47	-.47	-.44	-.37	-.22	.02	.38
118	110	.83	1.35	1.91	2.39	2.77	3.01	3.15	3.18	3.18	3.11	2.78	2.27	1.67	.74
119	111	-.19	-1.25	-2.33											
120	112	-.47	-.47	-.47	-.47	-.47	-.47	-.47	-.48	-.48	-.48	-.46	-.42	-.31	-.14



```

10/26/77 EXPJRT VCSA B33L CASL
JBAR      120   NDT      4000
DT         .100E+11DX   .300E+13 GROVEL   0.
RMIN      0.      RMAX    .156E+13
DJNR MASS .100E+01DJNR MUM .100E+01
GAMMA     .167E+01UTL   0.      UTMAX     0.
VLAM      J.      DTMAX   .100E+11 DTK     .200E+00
RATIO, RMAX FROM MESH GEN 1.00000000E+00 3.60000000E+14 3.00000000E+12
RATIO, RMAX FRJM MESH GEN 1.50000000E+00 3.20000000E+33 5.34091967E+32
RATIO, RMAX FROM MESH GEN 1.25000000E+00 3.34859587E+24 4.18574484E+23
RATIO, RMAX FROM MESH GEN 1.12000000E+00 2.74689621E+19 2.28908193E+18
RATIO, RMAX FRJM MESH GEN 1.06250000E+00 6.39254202E+16 3.19852101E+15
RATIO, RMAX FROM MESH GEN 1.09375000E+00 1.31528751E+18 8.96806708E+16
RATIO, RMAX FROM MESH GEN 1.07812500E+00 2.87955631E+17 1.71423233E+16
RATIO, RMAX FROM MESH GEN 1.07031250E+00 1.35305050E+17 7.42745396E+15
RATIO, RMAX FROM MESH GEN 1.07421375E+00 1.97281657E+17 1.12923683E+16
RATIO, RMAX FROM MESH GEN 1.07226562E+00 1.63356036E+17 9.15999748E+15
RATIO, RMAX FROM MESH GEN 1.07124906E+00 1.48664504E+17 8.24875514E+15
RATIO, RMAX FRJM MESH GEN 1.07177734E+00 1.55835727E+17 8.69254737E+15
RATIO, RMAX FRJM MESH GEN 1.07202149E+00 1.59551199E+17 8.92323859E+15
RATIO, RMAX FRJM MESH GEN 1.07184941E+00 1.57682425E+17 8.80714425E+15
RATIO, RMAX FROM MESH GEN 1.07183339E+00 1.56756333E+17 8.74965983E+15
RATIO, RMAX FRJM MESH GEN 1.07180785E+00 1.56295346E+17 8.72105726E+15
RATIO, RMAX FROM MESH GEN 1.07179260E+00 1.56065366E+17 8.70679075E+15
RATIO, RMAX FROM MESH GEN 1.07178497E+00 1.55950504E+17 8.69956661E+15
RATIO, RMAX FRJM MESH GEN 1.07178379E+00 1.56007224E+17 8.70322774E+15
1.00000420E+04

```

INTERNAL ENERGY =		-I TOTAL ENERGY =		-I MASS =		-I MOMENTUM =		-I CYCLE =		O	
J	X	U	R4D	EI	P	CND	L	MR	T		
2	0.	J.	2.22000E-19	2.61630E+08	4.39758E-11	-1.49992E+19	0.	0.	5.00001E+00		
3	3.00000E+12	J.	2.22000E-19	2.99006E+08	4.39758E-11	8.74058E+12	0.	2.85005E+19	5.71429E+00		
4	6.00000E+12	J.	1.39000E-19	3.46840E+08	4.39758E-11	6.31347E+12	0.	2.03066E+20	6.66667E+00		
5	9.21537E+12	0.	1.57500E-19	4.18808E+08	4.39758E-11	4.02691E+12	0.	6.51630E+20	8.00001E+00		
6	1.26616E+13	0.	1.26000E-19	5.23260E+08	4.39758E-11	1.39212E+12	0.	1.47448E+21	1.00000E+01		
7	1.63552E+13	0.	1.26000E-19	5.23260E+08	4.39758E-11	0.	0.	2.71215E+21	1.00000E+01		
8	2.03139E+13	0.	1.26000E-19	5.23260E+08	4.39758E-11	0.	0.	4.82740E+21	1.00000E+01		
9	2.45568E+13	0.	1.26000E-19	5.23260E+08	4.39758E-11	0.	0.	8.21902E+21	1.00000E+01		
10	2.91044E+13	0.	1.26000E-19	5.23260E+08	4.39758E-11	0.	0.	1.34149E+22	1.00000E+01		
11	3.37734E+13	0.	1.26000E-19	5.23260E+08	4.39758E-11	0.	0.	2.11078E+22	1.00000E+01		
12	3.82023E+13	0.	1.26000E-19	5.23260E+08	4.39758E-11	0.	0.	3.22007E+22	1.00000E+01		
13	4.48012E+13	0.	1.26000E-19	5.23260E+08	4.39758E-11	0.	0.	4.78632E+22	1.00000E+01		
14	5.08021E+13	0.	1.26000E-19	5.23260E+08	4.39758E-11	0.	0.	6.96027E+22	1.00000E+01		
15	5.72337E+13	0.	1.26000E-19	5.23260E+08	4.39758E-11	0.	0.	9.73530E+22	1.00000E+01		
16	6.41271E+13	J.	1.26000E-19	5.23260E+08	4.39758E-11	0.	0.	1.39585E+23	1.00000E+01		
17	7.15153E+13	0.	1.26000E-19	5.23260E+08	4.39758E-11	0.	0.	1.93447E+23	1.00000E+01		
18	7.94340E+13	J.	1.25000E-19	5.23260E+08	4.39758E-11	0.	0.	2.64935E+23	1.00000E+01		
19	8.77211E+13	0.	1.25000E-19	5.23260E+08	4.39758E-11	0.	0.	3.59109E+23	1.00000E+01		
20	9.70174E+13	0.	1.26000E-19	5.23260E+08	4.39758E-11	0.	0.	4.82361E+23	1.00000E+01		
21	1.06767E+14	0.	1.26000E-19	5.23260E+08	4.39758E-11	0.	0.	6.42748E+23	1.00000E+01		
22	1.17216E+14	0.	1.26000E-19	5.23260E+08	4.39758E-11	0.	0.	8.50408E+23	1.00000E+01		
23	1.28416E+14	0.	1.26000E-19	5.23260E+08	4.39758E-11	0.	0.	1.11807E+24	1.00000E+01		
24	1.40419E+14	0.	1.26000E-19	5.23260E+08	4.39758E-11	0.	0.	1.46169E+24	1.00000E+01		
25	1.53234E+14	0.	1.25000E-19	5.23260E+08	4.39758E-11	0.	0.	1.90127E+24	1.00000E+01		
26	1.67073E+14	0.	1.26000E-19	5.23260E+08	4.39758E-11	0.	0.	2.46177E+24	1.00000E+01		
27	1.81351E+14	J.	1.26000E-19	5.23260E+08	4.39758E-11	0.	0.	3.17442E+24	1.00000E+01		
28	1.97091E+14	0.	1.26000E-19	5.23260E+08	4.39758E-11	0.	0.	4.07815E+24	1.00000E+01		
29	2.14658E+14	0.	1.26000E-19	5.23260E+08	4.39758E-11	0.	0.	5.22146E+24	1.00000E+01		
30	2.32863E+14	J.	1.26000E-19	5.23260E+08	4.39758E-11	0.	0.	6.66480E+24	1.00000E+01		
31	2.52365E+14	J.	1.26000E-19	5.23260E+08	4.39758E-11	0.	0.	8.48330E+24	1.00000E+01		
32	2.73256E+14	0.	1.26000E-19	5.23260E+08	4.39758E-11	0.	0.	1.07704E+25	1.00000E+01		
33	2.95669E+14	J.	1.26000E-19	5.23260E+08	4.39758E-11	0.	0.	1.36422E+25	1.00000E+01		
34	3.19079E+14	0.	1.26000E-19	5.23260E+08	4.39758E-11	0.	0.	1.72429E+25	1.00000E+01		
35	3.45412E+14	0.	1.26000E-19	5.23260E+08	4.39758E-11	0.	0.	2.17511E+25	1.00000E+01		









102	4.777777E+16	-1.433294E+01	1.26001E-19	5.23263E+08	4.39766E-11	0.	0.	3.36377E+31	1.00001E+01
103	4.28146E+16	-1.53949E+01	1.26001E-19	5.23263E+08	4.39766E-11	0.	0.	4.14229E+31	1.00001E+01
104	4.58713E+16	-1.61795E+01	1.26001E-19	5.23263E+08	4.39766E-11	0.	0.	5.10091E+31	1.00001E+01
105	4.71893E+16	-1.7320E+01	1.26001E-19	5.23263E+08	4.39766E-11	0.	0.	6.28129E+31	1.00001E+01
106	5.27222E+16	-1.53779E+01	1.26001E-19	5.23263E+08	4.39766E-11	0.	0.	7.73473E+31	1.00001E+01
107	5.65079E+16	-1.99233E+01	1.26001E-19	5.23263E+08	4.39766E-11	0.	0.	9.52439E+31	1.00001E+01
108	6.05674E+16	-2.13546E+01	1.26001E-19	5.23263E+08	4.39766E-11	0.	0.	1.17280E+32	1.00001E+01
109	6.47204E+16	-2.28885E+01	1.26001E-19	5.23263E+08	4.39766E-11	0.	0.	1.44414E+32	1.00001E+01
110	6.95338E+16	-2.45327E+01	1.26001E-19	5.23263E+08	4.39766E-11	0.	0.	1.77823E+32	1.00001E+01
111	7.45319E+16	-2.52949E+01	1.26001E-19	5.23253E+08	4.39766E-11	0.	0.	2.18960E+32	1.00001E+01
112	7.99338E+16	-2.81337E+01	1.26001E-19	5.23263E+08	4.39766E-11	0.	0.	2.69611E+32	1.00001E+01
113	8.56803E+16	-3.02075E+01	1.26001E-19	5.23263E+08	4.39766E-11	0.	0.	3.31976E+32	1.00001E+01
114	9.18340E+16	-3.23773E+01	1.26001E-19	5.23263E+08	4.39766E-11	0.	0.	4.08765E+32	1.00001E+01
115	9.34274E+16	-3.47026E+01	1.26001E-19	5.23263E+08	4.39766E-11	0.	0.	5.03314E+32	1.00001E+01
116	1.05473E+17	-3.71949E+01	1.26001E-19	5.23263E+08	4.39766E-11	0.	0.	6.19727E+32	1.00001E+01
117	1.13075E+17	-3.98680E+01	1.26001E-19	5.23263E+08	4.39766E-11	0.	0.	7.63063E+32	1.00001E+01
118	1.21135E+17	-4.27339E+01	1.26001E-19	5.23263E+08	4.39766E-11	0.	0.	9.39546E+32	1.00001E+01
119	1.29898E+17	-4.57974E+01	1.26001E-19	5.23263E+08	4.39766E-11	0.	0.	1.15684E+33	1.00001E+01
120	1.38601E+17	-4.85658E+01	1.26001E-19	5.23263E+08	4.39766E-11	0.	0.	1.40529E+33	1.00001E+01
121	1.47305E+17	-5.18874E+01	1.26001E-19	5.23240E+08	4.39717E-11	0.	0.	1.68699E+33	9.99964E+00
122	1.56008E+17	0.	1.26001E-19	5.23260E+08	4.39717E-11	0.	0.	2.00401E+33	1.00000E+01
DT	0.93595150E+09	T	3.56029979E+10	5	1.26021E-19	-4.96740E-01	1.00000E+01		
DT	1.00000000E+10	T	8.3567973E+10	10	1.26037E-19	-1.43313E-01	1.00000E+01		
DT	1.00000000E+10	T	1.30356797E+11	15	1.26105E-19	-2.44042E-01	1.00000E+01		
DT	1.00000000E+10	T	1.60856797E+11	20	1.26205E-19	-3.45041E-01	1.00001E+01		
DT	1.00000000E+10	T	2.03056797E+11	25	1.26339E-19	-4.46353E-01	1.00000E+01		
DT	1.00000000E+10	T	2.60856797E+11	30	1.26508E-19	-5.47830E-01	1.00001E+01		
DT	1.00000000E+10	T	3.30856797E+11	35	1.26710E-19	-6.49583E-01	1.00000E+01		
DT	1.00000000E+10	T	3.80356797E+11	40	1.26946E-19	-7.51577E-01	1.00001E+01		
DT	1.00000000E+10	T	4.30356797E+11	45	1.27217E-19	-8.54008E-01	1.00001E+01		
DT	1.00000000E+10	T	4.80856797E+11	50	1.27522E-19	-9.56817E-01	1.00001E+01		
DT	1.00000000E+10	T	5.30856797E+11	55	1.27863E-19	-1.06002E+00	1.00001E+01		
DT	1.00000000E+10	T	5.80856797E+11	60	1.28240E-19	-1.16378E+00	1.00001E+01		
DT	1.00000000E+10	T	6.30356797E+11	65	1.28653E-19	-1.26804E+00	1.00001E+01		
DT	1.00000000E+10	T	6.90856797E+11	70	1.29103E-19	-1.37300E+00	1.00001E+01		
DT	1.00000000E+10	T	7.30856797E+11	75	1.29589E-19	-1.47856E+00	1.00001E+01		
DT	1.00000000E+10	T	7.80856797E+11	80	1.30114E-19	-1.58486E+00	1.00001E+01		
DT	1.00000000E+10	T	8.30856797E+11	85	1.30678E-19	-1.69192E+00	1.00001E+01		
DT	1.00000000E+10	T	8.80856797E+11	90	1.31281E-19	-1.79980E+00	1.00001E+01		
DT	1.00000000E+10	T	9.30856797E+11	95	1.31924E-19	-1.90877E+00	1.00001E+01		
DT	1.00000000E+10	T	9.80856797E+11	100	1.32609E-19	-2.01827E+00	1.00001E+01		
DT	1.00000000E+10	T	1.03085680E+12	105	1.33335E-19	-2.12898E+00	1.00001E+01		
DT	1.00000000E+10	T	1.08085680E+12	110	1.34105E-19	-2.24076E+00	1.00001E+01		
DT	1.00000000E+10	T	1.13085680E+12	115	1.34919E-19	-2.35368E+00	1.00001E+01		
DT	1.00000000E+10	T	1.18085680E+12	120	1.35778E-19	-2.46777E+00	1.00001E+01		
DT	1.00000000E+10	T	1.23085680E+12	125	1.36684E-19	-2.58317E+00	1.00001E+01		
DT	1.00000000E+10	T	1.28085680E+12	130	1.37638E-19	-2.69986E+00	1.00001E+01		
DT	1.00000000E+10	T	1.33085680E+12	135	1.38641E-19	-2.81799E+00	1.00001E+01		
DT	1.00000000E+10	T	1.38085680E+12	140	1.39695E-19	-2.93760E+00	1.00001E+01		
DT	1.00000000E+10	T	1.43085680E+12	145	1.40802E-19	-3.05876E+00	1.00001E+01		
DT	1.00000000E+10	T	1.48085680E+12	150	1.41963E-19	-3.18159E+00	1.00001E+01		
DT	1.00000000E+10	T	1.53085680E+12	155	1.43179E-19	-3.30612E+00	1.00001E+01		
DT	1.00000000E+10	T	1.58085680E+12	160	1.44454E-19	-3.43248E+00	1.00001E+01		
DT	1.00000000E+10	T	1.63085680E+12	165	1.45789E-19	-3.56074E+00	1.00001E+01		
DT	1.00000000E+10	T	1.68085680E+12	170	1.47179E-19	-3.69103E+00	1.00001E+01		
DT	1.00000000E+10	T	1.73085680E+12	175	1.48648E-19	-3.82339E+00	1.00001E+01		
DT	1.00000000E+10	T	1.78085680E+12	180	1.50177E-19	-3.95796E+00	1.00001E+01		
DT	1.00000000E+10	T	1.83085680E+12	185	1.51776E-19	-4.09485E+00	1.00001E+01		
DT	1.00000000E+10	T	1.88085680E+12	190	1.53448E-19	-4.23415E+00	1.00001E+01		
DT	1.00000000E+10	T	1.93085680E+12	195	1.55195E-19	-4.37602E+00	1.00001E+01		
DT	1.00000000E+10	T	1.98085680E+12	200	1.57021E-19	-4.52054E+00	1.00001E+01		
DT	1.00000000E+10	T	2.03085680E+12	205	1.58930E-19	-4.66786E+00	1.00001E+01		
DT	1.00000000E+10	T	2.08085680E+12	210	1.60925E-19	-4.81811E+00	1.00001E+01		

DT	1.00000000E+10	T	2.1308560E+12	215	1.63009E-19	-4.97145E+00	1.00001E+01
DT	1.00000000E+10	T	2.1800560E+12	220	1.65188E-19	-5.12901E+00	1.00001E+01
DT	1.00000000E+10	T	2.2308560E+12	225	1.67466E-19	-5.28795E+00	1.00001E+01
DT	1.00000000E+10	T	2.2808560E+12	230	1.69847E-19	-5.45145E+00	1.00001E+01
DT	1.00000000E+10	T	2.3308560E+12	235	1.72337E-19	-5.61567E+00	1.00001E+01
DT	1.00000000E+10	T	2.3808560E+12	240	1.74941E-19	-5.78931E+00	1.00001E+01
DT	1.00000000E+10	T	2.4308560E+12	245	1.77666E-19	-5.96506E+00	1.00002E+01
DT	1.00000000E+10	T	2.4808560E+12	250	1.80517E-19	-6.14463E+00	1.00002E+01
DT	1.00000000E+10	T	2.5308560E+12	255	1.83501E-19	-6.32875E+00	1.00002E+01
DT	1.00000000E+10	T	2.5808560E+12	260	1.86627E-19	-6.51763E+00	1.00002E+01
DT	1.00000000E+10	T	2.6308560E+12	265	1.89901E-19	-6.71154E+00	1.00002E+01
DT	1.00000000E+10	T	2.6808560E+12	270	1.93333E-19	-6.91074E+00	1.00002E+01
DT	1.00000000E+10	T	2.7308560E+12	275	1.96931E-19	-7.11550E+00	1.00002E+01
DT	1.00000000E+10	T	2.7808560E+12	280	2.00709E-19	-7.32612E+00	1.00002E+01
DT	1.00000000E+10	T	2.8308560E+12	285	2.04667E-19	-7.54293E+00	1.00002E+01
DT	1.00000000E+10	T	2.8808560E+12	290	2.08829E-19	-7.76628E+00	1.00002E+01
DT	1.00000000E+10	T	2.9308560E+12	295	2.13201E-19	-7.99651E+00	1.00002E+01
DT	1.00000000E+10	T	2.9808560E+12	300	2.17799E-19	-8.23403E+00	1.00002E+01
DT	1.00000000E+10	T	3.0308560E+12	305	2.22638E-19	-8.47921E+00	1.00002E+01
DT	1.00000000E+10	T	3.0808560E+12	310	2.27744E-19	-8.73256E+00	1.00002E+01
DT	1.00000000E+10	T	3.1308560E+12	315	2.33104E-19	-8.99453E+00	1.00002E+01
DT	1.00000000E+10	T	3.1808560E+12	320	2.38709E-19	-9.26554E+00	1.00002E+01
DT	1.00000000E+10	T	3.2308560E+12	325	2.44748E-19	-9.54645E+00	1.00002E+01
DT	1.00000000E+10	T	3.2808560E+12	330	2.51067E-19	-9.83756E+00	1.00002E+01
DT	1.00000000E+10	T	3.3308560E+12	335	2.57750E-19	-1.01396E+01	1.00002E+01
DT	1.00000000E+10	T	3.3808560E+12	340	2.64825E-19	-1.04534E+01	1.00002E+01
DT	1.00000000E+10	T	3.4308560E+12	345	2.72324E-19	-1.07795E+01	1.00002E+01
DT	1.00000000E+10	T	3.4808560E+12	350	2.80280E-19	-1.11189E+01	1.00002E+01
DT	1.00000000E+10	T	3.5308560E+12	355	2.88733E-19	-1.14725E+01	1.00002E+01
DT	1.00000000E+10	T	3.5808560E+12	360	2.97724E-19	-1.18412E+01	1.00002E+01
DT	1.00000000E+10	T	3.6308560E+12	365	3.07249E-19	-1.22261E+01	1.00003E+01
DT	1.00000000E+10	T	3.6808560E+12	370	3.17512E-19	-1.26284E+01	1.00003E+01
DT	1.00000000E+10	T	3.7308560E+12	375	3.28420E-19	-1.30494E+01	1.00003E+01
DT	1.00000000E+10	T	3.7808560E+12	380	3.40089E-19	-1.34905E+01	1.00003E+01
DT	1.00000000E+10	T	3.8308560E+12	385	3.52593E-19	-1.39532E+01	1.00003E+01
DT	1.00000000E+10	T	3.8808560E+12	390	3.66014E-19	-1.44394E+01	1.00003E+01
DT	1.00000000E+10	T	3.9308560E+12	395	3.80446E-19	-1.49508E+01	1.00003E+01
DT	1.00000000E+10	T	3.9808560E+12	400	3.95995E-19	-1.54896E+01	1.00003E+01
DT	1.00000000E+10	T	4.0308560E+12	405	4.12782E-19	-1.60580E+01	1.00003E+01
DT	1.00000000E+10	T	4.0808560E+12	410	4.30946E-19	-1.66587E+01	1.00003E+01
DT	1.00000000E+10	T	4.1308560E+12	415	4.50643E-19	-1.72943E+01	1.00003E+01
DT	1.00000000E+10	T	4.1808560E+12	420	4.72055E-19	-1.79678E+01	1.00003E+01
DT	1.00000000E+10	T	4.2308560E+12	425	4.95392E-19	-1.86824E+01	1.00004E+01
DT	1.00000000E+10	T	4.2808560E+12	430	5.20895E-19	-1.94414E+01	1.00004E+01
DT	1.00000000E+10	T	4.3308560E+12	435	5.48845E-19	-2.02478E+01	1.00004E+01
DT	1.00000000E+10	T	4.3808560E+12	440	5.79567E-19	-2.11046E+01	1.00004E+01
DT	1.00000000E+10	T	4.4308560E+12	445	6.13437E-19	-2.20140E+01	1.00004E+01
DT	1.00000000E+10	T	4.4808560E+12	450	6.50896E-19	-2.29769E+01	1.00004E+01
DT	1.00000000E+10	T	4.5308560E+12	455	6.92448E-19	-2.39916E+01	1.00004E+01
DT	1.00000000E+10	T	4.5808560E+12	460	7.38675E-19	-2.50537E+01	1.00005E+01
DT	1.00000000E+10	T	4.6308560E+12	465	7.90241E-19	-2.61534E+01	1.00005E+01
DT	1.00000000E+10	T	4.6808560E+12	470	8.47886E-19	-2.72745E+01	1.00005E+01
DT	1.00000000E+10	T	4.7308560E+12	475	9.12421E-19	-2.83919E+01	1.00005E+01
DT	1.00000000E+10	T	4.7808560E+12	480	9.84705E-19	-2.94700E+01	1.00005E+01
DT	1.00000000E+10	T	4.8308560E+12	485	1.06560E-18	-3.04622E+01	1.00005E+01
DT	1.00000000E+10	T	4.8808560E+12	490	1.15591E-18	-3.13107E+01	1.00006E+01
DT	1.00000000E+10	T	4.9308560E+12	495	1.25627E-18	-3.19505E+01	1.00006E+01
DT	1.00000000E+10	T	4.9808560E+12	500	1.36707E-18	-3.23148E+01	1.00006E+01

INTERNAL ENERGY = 1.0448531E+42 TOTAL ENERGY = 1.113411E+42 MASS = 2.004007E+33 MOMENTUM = -2.915586E+37 CYCLE = 500

J	X	J	RHD	LI	P	CND	L	MR	T
2	0.	0.	1.39050E-13	5.23272E+18	4.80334E-10	3.56039E+14	0.	0.	1.00006E+01
3	3.00000E+12	-1.70270E+00	1.39050E-18	5.23292E+04	4.85334E-10	3.56038E+14	9.24645E+16	1.257201E+20	1.00006E+01
4	6.00000E+12	-3.39700E+00	1.39050E-18	5.23292E+08	4.85334E-10	3.56037E+14	7.39694E+17	1.25809E+21	1.00006E+01









APPENDIX B



```
*IDENT FIX
*DELETE SV.23
  DATA LFILM,KPR,NM/10,1,20/
*DELETE SV.313
  DATA (RCV(J),J=1,200)/200*8.02232E-09/
*DELETE SV.370,SV.373
  RHO(J)=2.4E-09
  P(J)=1.99543E+03
  IF (J .LE. 5) P(J)=5.37152E+14
*DELETE SV.613,SV.624
  CND(J)=0.5*(MUVISC(J-1)+MUVISC(J))/PR
*DELETE SV.611
  DATA PR/100./
*DELETE SV.616,SV.617
  MUVISC(J)=2.4E+07
*DELETE SV.527
*DELETE SV.78
*INSERT SV.509
  IF (IUMAX .GT. -1) RETURN
*INSERT SV.26
  G=0.
*DELETE SV.22
  DATA PDVCEN/0.51/
*INSERT SV.26
  CALL UNDROP
```

```

1 10/26/77 EXPORT VEGA BLAST WAVE
2 JBAR          60      NDT          300
3 DT           4.000E-001 DX          1.667E+011 GRDVEL          0.0
4 RMIN          0.000E+000 RMAX        9.000E+012
5 DONR MASS     1.00      DONR MOM     1.00
6 GAMMA         1.667 UT1              UTMAX
7 VLAM          0.2      DTMAX        +8.000E-01 DTK          0.20
8 .70000 .27000
9 1-4.48-3.80-3.20-2.86-2.72-2.67-2.64-2.63-2.63-2.62-2.62-2.62-2.61-2.60
10 2-2.60-2.59-2.58-2.55-2.54-2.52-2.49-2.46-2.42-5.54-4.59-4.59-4.59-4.59
11 3-4.59-4.59-4.59
12 4-4.73-4.71-4.59-4.14-3.52-3.04-2.80-2.69-2.55-2.63-2.61-2.60-2.59-2.57
13 5-2.55-2.52-2.49-2.44-2.39-2.33-2.26-2.18-2.09-5.32-4.41-4.41-4.41-4.41
14 6-4.41-4.41-4.41
15 7-4.53-4.51-4.48-4.41-4.29-4.05-3.60-3.12-2.83-2.69-2.62-2.57-2.53-2.48
16 8-2.43-2.36-2.29-2.20-2.09-1.98-1.85-1.72-1.58-5.09-4.23-4.23-4.23-4.23
17 9-4.23-4.23-4.23
18 10-4.44-4.41-4.38-4.31-4.21-4.08-3.90-3.64-3.28-2.90-2.60-2.41-2.25-2.13
19 11-2.01-1.88-1.73-1.59-1.43-1.28-1.12 -.96 -.80-4.87-4.05-4.05-4.05-4.05
20 12-4.05-4.05-4.05
21 13-4.31-4.29-4.32-4.24-4.10-3.92-3.68-3.39-3.06-2.72-2.38-2.07-1.82-1.62
22 14-1.45-1.27-1.08 -.90 -.71 -.52 -.33 -.14 .00-4.65-3.87-3.87-3.87-3.87
23 15-3.87-3.87-3.87
24 16-4.13-4.14-4.23-4.12-3.94-3.68-3.37-3.04-2.69-2.35-2.03-1.72-1.44-1.20
25 17 -.98 -.76 -.53 -.30 -.08 .15 .38 .61 .66-4.43-3.70-3.70-3.70-3.70
26 18-3.70-3.70-3.70
27 19-3.96-3.99-4.03-3.92-3.71-3.39-3.03-2.69-2.35-2.04-1.73-1.43-1.13 -.86
28 20 -.60 -.33 -.06 .21 .47 .74 1.01 1.26 1.06-4.21-3.52-3.52-3.52-3.52
29 21-3.52-3.52-3.52
30 22-3.31-3.40-3.56-3.52-3.37-3.12-2.82-2.51-2.17-1.82-1.47-1.13 -.80 -.51
31 23 -.24 .05 .33 .51 .89 1.17 1.46 1.72 1.25-3.99-3.34-3.34-3.34-3.34
32 24-3.34-3.34-3.34
33 25-2.63-2.79-2.95-2.98-2.93-2.78-2.55-2.28-1.96-1.59-1.21 -.84 -.50 -.20
34 26 .08 .37 .66 .96 1.25 1.54 1.83 2.08 1.39-3.77-3.16-3.16-3.16-3.16
35 27-3.16-3.16-3.16
36 28-1.90-2.06-2.24-2.37-2.39-2.27-2.06-1.81-1.53-1.23 -.91 -.58 -.26 .05
37 29 .35 .67 .98 1.29 1.60 1.91 2.22 2.45 1.51-3.55-2.98-2.98-2.98-2.98
38 30-2.98-2.98-2.98
39 31-1.27-1.39-1.49-1.61-1.66-1.56-1.39-1.18 -.96 -.72 -.47 -.20 .09 .38
40 32 .68 .97 1.28 1.58 1.88 2.18 2.47 2.65 1.61-3.33-2.80-2.80-2.80-2.80

```

41	33-2.80-2.80-2.80
42	34 -.79 -.79 -.77 -.79 -.80 -.73 -.62 -.47 -.30 -.10 .11 .33 .56 .81
43	35 1.05 1.32 1.59 1.85 2.12 2.38 2.64 2.78 1.71-3.11-2.62-2.62-2.52-2.62
44	36-2.62-2.52-2.62
45	37 -.40 -.32 -.23 -.16 -.08 -.01 .07 .19 .33 .49 .57 .86 1.06 1.29
46	38 1.52 1.76 2.01 2.25 2.49 2.73 2.96 3.01 1.82-2.89-2.44-2.44-2.44-2.44
47	39-2.44-2.44-2.44
48	40 -.44 -.26 -.07 .18 .42 .59 .74 .86 .97 1.10 1.24 1.39 1.55 1.76
49	41 1.37 2.18 2.40 2.62 2.83 3.05 3.25 3.19 1.92-2.66-2.26-2.26-2.26-2.26
50	42-2.26-2.26-2.26
51	43 -.47 -.28 -.08 .22 .55 .89 1.19 1.39 1.54 1.66 1.77 1.90 2.05 2.21
52	44 2.38 2.58 2.78 2.97 3.17 3.36 3.52 3.35 2.02-2.44-2.08-2.08-2.08-2.08
53	45-2.08-2.08-2.08
54	46 -.47 -.40 -.31 .01 .43 .86 1.28 1.62 1.90 2.09 2.24 2.37 2.50 2.63
55	47 2.78 2.95 3.12 3.31 3.49 3.67 3.80 3.49 2.12-2.22-1.90-1.90-1.90-1.90
56	48-1.90-1.90-1.90
57	49 -.47 -.47 -.48 -.18 .24 .68 1.14 1.59 2.00 2.31 2.56 2.74 2.88 3.01
58	50 3.14 3.28 3.44 3.60 3.78 3.97 4.07 3.62 2.23-2.00-1.72-1.72-1.72-1.72
59	51-1.72-1.72-1.72
60	52 -.47 -.47 -.49 -.25 .09 .49 .93 1.42 1.90 2.33 2.69 2.96 3.15 3.32
61	53 3.45 3.58 3.72 3.87 4.04 4.23 4.30 3.73 2.33-1.78-1.54-1.54-1.54-1.54
62	54-1.54-1.54-1.54
63	55 -.47 -.47 -.47 -.30 -.04 .29 .70 1.19 1.71 2.22 2.68 3.04 3.32 3.54
64	56 3.71 3.85 3.98 4.12 4.28 4.43 4.43 3.80 2.43-1.56-1.36-1.36-1.36-1.36
65	57-1.36-1.36-1.36
66	58 -.47 -.47 -.47 -.35 -.15 .15 .53 1.01 1.53 2.07 2.58 3.01 3.37 3.66
67	59 3.89 4.07 4.21 4.36 4.50 4.57 4.49 3.86 2.52-1.34-1.19-1.19-1.19-1.19
68	60-1.19-1.19-1.19
69	61 -.47 -.47 -.47 -.39 -.23 .03 .38 .83 1.34 1.89 2.43 2.91 3.33 3.71
70	62 4.02 4.24 4.41 4.58 4.70 4.70 4.53 3.92 2.52-1.12-1.01-1.01-1.01-1.01
71	63-1.01-1.01-1.01
72	64 -.47 -.47 -.47 -.40 -.26 -.04 .27 .69 1.18 1.73 2.28 2.79 3.26 3.69
73	65 4.06 4.34 4.57 4.78 4.92 4.94 4.72 4.02 2.72 -.90 -.83 -.83 -.83 -.83
74	66 -.83 -.83 -.83
75	67 -.47 -.47 -.47 -.40 -.28 -.10 .17 .56 1.04 1.57 2.13 2.66 3.17 3.64
76	68 4.05 4.41 4.69 4.94 5.11 5.14 4.87 4.11 2.82 -.68 -.65 -.65 -.65 -.65
77	69 -.65 -.65 -.65
78	70 -.47 -.47 -.47 -.41 -.29 -.14 .09 .46 .91 1.43 1.99 2.53 3.05 3.56
79	71 4.02 4.43 4.77 5.06 5.27 5.32 5.00 4.19 2.93 -.46 -.47 -.47 -.47 -.47
80	72 -.47 -.47 -.47

81	73	-.47	-.47	-.47	-.42	-.32	-.18	.03	.38	.82	1.33	1.88	2.42	2.95	3.46
82	74	3.95	4.40	4.79	5.11	5.35	5.41	5.08	4.27	3.03	-.24	-.29	-.29	-.29	-.29
83	75	-.29	-.29	-.29											
84	76	-.47	-.47	-.47	-.44	-.36	-.23	-.02	.32	.75	1.26	1.80	2.33	2.85	3.38
85	77	3.88	4.34	4.76	5.10	5.34	5.39	5.09	4.33	3.12	-.01	-.11	-.11	-.11	-.11
86	78	-.11	-.11	-.11											
87	79	-.47	-.47	-.47	-.46	-.40	-.28	-.07	.26	.68	1.18	1.72	2.24	2.75	3.28
88	80	3.78	4.26	4.68	5.05	5.30	5.32	5.07	4.38	3.22	.21	.07	.07	.07	.07
89	81	.07	.07	.07											
90	82	-.47	-.47	-.47	-.47	-.44	-.32	-.12	.20	.60	1.10	1.63	2.14	2.65	3.16
91	83	3.67	4.15	4.58	4.95	5.20	5.22	5.00	4.42	3.32	.43	.25	.25	.25	.25
92	84	.25	.25	.25											
93	85	-.47	-.47	-.47	-.49	-.47	-.36	-.16	.14	.52	1.00	1.52	2.02	2.52	3.04
94	86	3.54	4.01	4.44	4.82	5.07	5.06	4.88	4.43	3.41	.65	.43	.43	.43	.43
95	87	.43	.43	.43											
96	88	-.47	-.47	-.47	-.49	-.48	-.39	-.23	.01	.35	.80	1.31	1.82	2.34	2.87
97	89	3.39	3.87	4.30	4.67	4.92	4.93	4.81	4.45	3.51	.87	.61	.61	.61	.61
98	90	.61	.61	.61											
99	91	-.47	-.47	-.47	-.49	-.48	-.42	-.30	-.11	.17	.60	1.10	1.61	2.15	2.70
100	92	3.22	3.71	4.14	4.50	4.75	4.80	4.73	4.46	3.60	1.09	.79	.79	.79	.79
101	93	.79	.79	.79											
102	94	-.47	-.47	-.47	-.48	-.47	-.44	-.36	-.22	.01	.39	.87	1.39	1.94	2.50
103	95	3.04	3.54	3.97	4.34	4.59	4.58	4.66	4.47	3.69	1.31	.97	.97	.97	.97
104	96	.97	.97	.97											
105	97	-.47	-.47	-.47	-.48	-.47	-.46	-.41	-.30	-.09	.25	.68	1.18	1.72	2.29
105	98	2.85	3.36	3.81	4.19	4.47	4.58	4.59	4.44	3.77	1.53	1.15	1.15	1.15	1.15
107	99	1.15	1.15	1.15											
108	100	-.47	-.47	-.47	-.47	-.47	-.47	-.44	-.35	-.17	.12	.51	.98	1.50	2.07
109	101	2.54	3.17	3.65	4.05	4.35	4.49	4.52	4.39	3.82	1.75	1.32	1.32	1.32	1.32
110	102	1.32	1.32	1.32											
111	103	-.47	-.47	-.47	-.47	-.47	-.49	-.47	-.39	-.23	.01	.34	.78	1.29	1.85
112	104	2.43	2.98	3.48	3.91	4.23	4.39	4.43	4.30	3.84	1.97	1.50	1.20	.71	-.27
113	105	-1.20	-2.29	-3.39											
114	106	-.47	-.47	-.47	-.47	-.47	-.48	-.49	-.46	-.40	-.30	-.13	.16	.56	1.07
115	107	1.63	2.22	2.76	3.21	3.54	3.74	3.82	3.79	3.65	2.79	2.20	1.75	1.19	.24
116	108	-.70	-1.77	-2.86											
117	109	-.47	-.47	-.47	-.47	-.47	-.47	-.47	-.47	-.47	-.44	-.37	-.22	.02	.38
118	110	.83	1.36	1.91	2.39	2.77	3.01	3.15	3.18	3.18	3.11	2.78	2.27	1.67	.74
119	111	-.19	-1.25	-2.33											
120	112	-.47	-.47	-.47	-.47	-.47	-.47	-.47	-.48	-.48	-.48	-.46	-.42	-.31	-.14



APPENDIX C

```
1 *IDENT PR0B
2 *DELETE SV.23
3     DATA LFILM,KPR,NM/50,5,200/
4 *DELETE SV.313
5     DATA (RCV(J),J=1,200)/200*4.E-09/
6 *DELETE SV.259
7     U(JP2)=U(JP1)+DELU
8     U(JP3)=U(JP2)+DELU
9     RHO(1)=3.674E-21
10    EI(JP2)=2.*EI(JP1)-EI(JBAR)
11 *DELETE SV.261
12    EI(1)=2.65E+14
13 *DELETE SV.370,SV.373
14    RHO(J)=3.674E-21
15    EI(J)=2.65E+14
16    P(J)=(GAMMA-1.)*RHO(J)*EI(J)
17 *DELETE SV.375
18 *DELETE SV.618,SV.624
19    CND(J)=0.5*(MUVISC(J)+MUVISC(J-1))/PR
20 *DELETE SV.180
21    AA(K+1,L-5)=-1.
22 *DELETE SV.78
23 *DELETE SV.527
24 *DELETE SV.228
25 *DELETE SV.374
26    U(J)=UT1
27 *DELETE SV.87
28    SUM=1.33E+26
29 *DELETE SV.90
30    DPHI(JP2)=SUM/X(JP2)**2
31 *DELETE SV.204
32    RHOL(1)=3.674E-21
33    EI(1)=2.65E+14
34    UT(JP2)=UT(JP1)+DELU
35    UT(JP3)=UT(JP2)+DELU
36    EI(JP2)=2.*EI(JP1)-EI(JBAR)
37 *DELETE SV.552
38    DO 10 J=2,JP3
39 *INSERT SV.296
40    SUBROUTINE ASOLN(X,P,EI,RHO,U,GAMMA,JP1)
```

```

41     DIMENSION X(1),P(1),EI(1),RHO(1),U(1)
42     JP2=JP1+1
43     GNOT=1.33E+26
44     ANA=RHO(1)*U(2)*X(2)*X(2)
45     ANB=EI(1)+0.5*U(2)*U(2)+P(1)/RHO(1)-GNOT/X(2)
46     ANC=P(1)/RHO(1)**GAMMA
47     D2=GAMMA*ANC/(GAMMA-1.)
48     D3=GAMMA-1.
49     D4=SQRT(ANA**2*0.5)
50     WRITE (6,6) ANA,ANB,ANC,D2,D3,D4
51     6 FORMAT (1X,*A AND D*,7E15.6)
52     DO 1 J=3,JP2
53     ROLD=RHO(J)
54     DO 2 IT=1,200
55     RHO(J)=D4/(X(J)*X(J)*SQRT(ANB-D2*RHO(J)**D3+GNOT/X(J)))
56     IF (ABS(RHO(J)-ROLD) .LE. 1.E-10*ROLD) GO TO 3
57     ROLD=RHO(J)
58     2 CONTINUE
59     WRITE (6,4) J,ROLD,RHO(J)
60     4 FORMAT (1X,*ITER FAILURE*,I5,2E15.6)
61     3 CONTINUE
62     P(J)=ANC*RHO(J)**GAMMA
63     EI(J)=P(J)/(D3*RHO(J))
64     U(J)=ANA/(X(J)*X(J)*RHO(J))
65     WRITE (5,5) J,RHO(J),P(J),EI(J),U(J)
66     5 FORMAT (1X,*A SOLN*,I5,4E13.6)
67     END FILE 6
68     1 CONTINUE
69     RETURN
70     END
71 *INSERT SV.376
72     CALL ASOLN (X,P,EI,RHO,U,GAMMA,JP1)
73 *DELETE SV.511
74     DATA PR/1.E+05/
75 *INSERT SV.27
76     DELU=U(JP2)-U(JP1)
77 *DELETE SV.185
78     B(K+1)=DELU
79 *INSERT SV.617
80     $ *1.E-12

```



```
81 *DELETE SV.132
82     AA(4,7)=X(2)*X(2)
83     AA(4,12)=-X(3)*X(3)
84 *DELETE SV.229
85 *INSERT SV.210
86     RHOT=RHOL(J)
87     EIT=EI(J)
88     IF (J.NE. 2) GO TO 151
89     RHOT=RHOL(1)
90     EIT=EI(1)
91     151 CONTINUE
92 *DELETE SV.214
93     1RHOT)-UD(J+1)*AJ(J+1)*((1.+DUB2)*RHOL(J)+(1.-DUB2)*RHOL(J+1)))
94 *DELETE SV.215
95     1+(1.-DUB1)*RHOT*EIT)-UD(J+1)*AJ(J+1)*((1.+DUB2)*RHOL(J)*EI(J)
96 *IDENT SHOK
97 *INSERT PRJB.10
98     IF (T.LT.TSHOK .OR. T.GE.TSHJK+7560.) GO TO 1006
99     RHOL(1)=RHOL(1)*3.864
100     EI(1)=EI(1)*25.47
101     UT(2)=1.57E+08
102     1006 CONTINUE
103 *INSERT PRJB.26
104     IF (T.LT.TSHOK .OR. T.GE.TSHOK+7560.) GO TO 1007
105     RHOL(1)=RHOL(1)*3.864
106     EI(1)=EI(1)*25.47
107     U(2)=1.57E+08
108     1007 CONTINUE
109 *INSERT SV.22
110     DATA TSHOK/2.E+05/
111 *IDENT RADCO
112 *DELETE PRJB.22,PRJB.23
113     U(JP3)=U(JP2)
114 *DELETE PRJB.11,PRJB.12
115     UT(JP3)=UT(JP2)
116 *DELETE PRJB.7
117     AA(K+1,L-5)=-DT*U(JP2)/(X(JP2)-X(JP1))
118 *DELETE SV.184
119     AA(K+1,L)=1.-AA(K+1,L-5)
120 *DELETE PRJB.8
```

```
121      B(K+1)=U(JP2)
122 *INSERT SV.26
123      CALL UNDRDP
```

```

1 10/26/77 EXPORT VEGA SOLAR WIND
2 JBAR      140      NDT      5000
3 DT        1.000E+002 DX      1.500E+010 GRDVEL      0.0
4 RMIN      1.250E+012 RMAX    2.000E+013
5 DDNR MASS 0.50      DDNR MOM 0.50
6 GAMMA     1.667 UTI      +3.140E+07 UTMAX
7 VLAM      0.2      DTMAX    +1.000E+04 DTK      0.20
8 .70000 .27000
9 1-4.48-3.80-3.20-2.86-2.72-2.67-2.64-2.63-2.63-2.62-2.62-2.62-2.51-2.60
10 2-2.60-2.59-2.58-2.56-2.54-2.52-2.49-2.46-2.42-5.54-4.59-4.59-4.59-4.59
11 3-4.59-4.59-4.59
12 4-4.73-4.71-4.59-4.14-3.52-3.04-2.80-2.69-2.65-2.63-2.61-2.60-2.59-2.57
13 5-2.55-2.52-2.49-2.44-2.39-2.33-2.26-2.18-2.09-5.32-4.41-4.41-4.41-4.41
14 6-4.41-4.41-4.41
15 7-4.53-4.51-4.48-4.41-4.29-4.05-3.60-3.12-2.83-2.69-2.62-2.57-2.53-2.48
16 8-2.43-2.36-2.29-2.20-2.09-1.98-1.85-1.72-1.58-5.09-4.23-4.23-4.23-4.23
17 9-4.23-4.23-4.23
18 10-4.44-4.41-4.38-4.31-4.21-4.08-3.90-3.54-3.28-2.90-2.60-2.41-2.25-2.13
19 11-2.01-1.88-1.73-1.59-1.43-1.28-1.12 -.96 -.80-4.87-4.05-4.05-4.05-4.05
20 12-4.05-4.05-4.05
21 13-4.31-4.29-4.32-4.24-4.10-3.92-3.68-3.39-3.06-2.72-2.38-2.07-1.82-1.62
22 14-1.45-1.27-1.08 -.90 -.71 -.52 -.33 -.14 .00-4.65-3.87-3.87-3.87-3.87
23 15-3.87-3.87-3.87
24 16-4.13-4.14-4.23-4.12-3.94-3.68-3.37-3.04-2.69-2.35-2.03-1.72-1.44-1.20
25 17 -.98 -.76 -.53 -.30 -.08 .15 .38 .61 .66-4.43-3.70-3.70-3.70-3.70
26 18-3.70-3.70-3.70
27 19-3.96-3.99-4.03-3.92-3.71-3.39-3.03-2.69-2.35-2.04-1.73-1.43-1.13 -.86
28 20 -.60 -.33 -.06 .21 .47 .74 1.01 1.26 1.06-4.21-3.52-3.52-3.52-3.52
29 21-3.52-3.52-3.52
30 22-3.31-3.40-3.56-3.52-3.37-3.12-2.82-2.51-2.17-1.82-1.47-1.13 -.80 -.51
31 23 -.24 .05 .33 .61 .89 1.17 1.46 1.72 1.25-3.99-3.34-3.34-3.34-3.34
32 24-3.34-3.34-3.34
33 25-2.63-2.79-2.95-2.98-2.93-2.78-2.55-2.28-1.96-1.59-1.21 -.84 -.50 -.20
34 26 .08 .37 .66 .96 1.25 1.54 1.83 2.08 1.39-3.77-3.16-3.16-3.16-3.16
35 27-3.16-3.16-3.16
36 28-1.90-2.06-2.24-2.37-2.39-2.27-2.06-1.81-1.53-1.23 -.91 -.58 -.26 .05
37 29 .35 .57 .98 1.29 1.60 1.91 2.22 2.45 1.51-3.55-2.98-2.98-2.98-2.98
38 30-2.98-2.98-2.98
39 31-1.27-1.39-1.49-1.61-1.66-1.56-1.39-1.18 -.96 -.72 -.47 -.20 .09 .38
40 32 .63 .97 1.28 1.58 1.88 2.18 2.47 2.66 1.61-3.33-2.80-2.80-2.80-2.80

```

41	33	-2.80	-2.80	-2.80															
42	34	-.79	-.79	-.77	-.79	-.80	-.73	-.62	-.47	-.30	-.10	.11	.33	.56	.81				
43	35	1.05	1.32	1.59	1.85	2.12	2.38	2.64	2.78	1.71	-3.11	-2.62	-2.62	-2.62	-2.62				
44	36	-2.62	-2.62	-2.62															
45	37	-.40	-.32	-.23	-.16	-.08	-.01	.07	.19	.33	.49	.67	.86	1.06	1.29				
46	38	1.52	1.76	2.01	2.25	2.49	2.73	2.96	3.01	1.82	-2.89	-2.44	-2.44	-2.44	-2.44				
47	39	-2.44	-2.44	-2.44															
48	40	-.44	-.26	-.07	.18	.42	.59	.74	.86	.97	1.10	1.24	1.39	1.56	1.76				
49	41	1.97	2.18	2.40	2.62	2.83	3.05	3.25	3.19	1.92	-2.66	-2.26	-2.26	-2.26	-2.26				
50	42	-2.26	-2.26	-2.26															
51	43	-.47	-.28	-.08	.22	.55	.89	1.19	1.39	1.54	1.66	1.77	1.90	2.05	2.21				
52	44	2.38	2.58	2.78	2.97	3.17	3.36	3.52	3.35	2.02	-2.44	-2.08	-2.08	-2.08	-2.08				
53	45	-2.08	-2.08	-2.08															
54	46	-.47	-.40	-.31	.01	.43	.86	1.28	1.62	1.90	2.09	2.24	2.37	2.50	2.63				
55	47	2.78	2.95	3.12	3.31	3.49	3.67	3.86	3.49	2.12	-2.22	-1.90	-1.90	-1.90	-1.90				
56	48	-1.90	-1.90	-1.90															
57	49	-.47	-.47	-.48	-.18	.24	.68	1.14	1.59	2.00	2.31	2.56	2.74	2.88	3.01				
58	50	3.14	3.28	3.44	3.60	3.78	3.97	4.07	3.62	2.23	-2.00	-1.72	-1.72	-1.72	-1.72				
59	51	-1.72	-1.72	-1.72															
60	52	-.47	-.47	-.49	-.26	.09	.49	.93	1.42	1.90	2.33	2.69	2.96	3.16	3.32				
61	53	3.45	3.58	3.72	3.87	4.04	4.23	4.30	3.73	2.33	-1.78	-1.54	-1.54	-1.54	-1.54				
62	54	-1.54	-1.54	-1.54															
63	55	-.47	-.47	-.47	-.30	-.04	.29	.70	1.19	1.71	2.22	2.68	3.04	3.32	3.54				
64	56	3.71	3.85	3.98	4.12	4.28	4.43	4.43	3.80	2.43	-1.56	-1.36	-1.36	-1.36	-1.36				
65	57	-1.36	-1.36	-1.36															
66	58	-.47	-.47	-.47	-.35	-.15	.15	.53	1.01	1.53	2.07	2.58	3.01	3.37	3.66				
67	59	3.89	4.07	4.21	4.36	4.50	4.57	4.49	3.86	2.52	-1.34	-1.19	-1.19	-1.19	-1.19				
68	60	-1.19	-1.19	-1.19															
69	61	-.47	-.47	-.47	-.39	-.23	.03	.38	.83	1.34	1.89	2.43	2.91	3.33	3.71				
70	62	4.02	4.24	4.41	4.58	4.70	4.70	4.53	3.92	2.62	-1.12	-1.01	-1.01	-1.01	-1.01				
71	63	-1.01	-1.01	-1.01															
72	64	-.47	-.47	-.47	-.40	-.26	-.04	.27	.69	1.18	1.73	2.28	2.79	3.26	3.69				
73	65	4.06	4.34	4.57	4.78	4.92	4.94	4.72	4.02	2.72	-.90	-.83	-.83	-.83	-.83				
74	66	-.83	-.83	-.83															
75	67	-.47	-.47	-.47	-.40	-.28	-.10	.17	.55	1.04	1.57	2.13	2.66	3.17	3.64				
76	68	4.06	4.41	4.69	4.94	5.11	5.14	4.87	4.11	2.82	-.68	-.65	-.65	-.65	-.65				
77	69	-.65	-.65	-.65															
78	70	-.47	-.47	-.47	-.41	-.29	-.14	.09	.46	.91	1.43	1.99	2.53	3.05	3.56				
79	71	4.02	4.43	4.77	5.06	5.27	5.32	5.00	4.19	2.93	-.46	-.47	-.47	-.47	-.47				
80	72	-.47	-.47	-.47															

81	73	-.47	-.47	-.47	-.42	-.32	-.18	.03	.38	.82	1.33	1.88	2.42	2.95	3.46
82	74	3.95	4.40	4.79	5.11	5.35	5.41	5.08	4.27	3.03	-.24	-.29	-.29	-.29	-.29
83	75	-.29	-.29	-.29											
84	76	-.47	-.47	-.47	-.44	-.36	-.23	-.02	.32	.75	1.26	1.80	2.33	2.86	3.38
85	77	3.88	4.34	4.76	5.10	5.34	5.39	5.09	4.33	3.12	-.01	-.11	-.11	-.11	-.11
86	78	-.11	-.11	-.11											
87	79	-.47	-.47	-.47	-.46	-.40	-.28	-.07	.26	.68	1.18	1.72	2.24	2.76	3.28
88	80	3.78	4.26	4.68	5.05	5.30	5.32	5.07	4.38	3.22	.21	.07	.07	.07	.07
89	81	.07	.07	.07											
90	82	-.47	-.47	-.47	-.47	-.44	-.32	-.12	.20	.60	1.10	1.63	2.14	2.65	3.16
91	83	3.67	4.15	4.58	4.95	5.20	5.22	5.00	4.42	3.32	.43	.25	.25	.25	.25
92	84	.25	.25	.25											
93	85	-.47	-.47	-.47	-.49	-.47	-.36	-.16	.14	.52	1.00	1.52	2.02	2.52	3.04
94	86	3.54	4.01	4.44	4.82	5.07	5.06	4.88	4.43	3.41	.65	.43	.43	.43	.43
95	87	.43	.43	.43											
96	88	-.47	-.47	-.47	-.49	-.48	-.39	-.23	.01	.35	.80	1.31	1.82	2.34	2.87
97	89	3.39	3.87	4.30	4.67	4.92	4.93	4.81	4.45	3.51	.87	.61	.61	.61	.61
98	90	.61	.61	.61											
99	91	-.47	-.47	-.47	-.49	-.48	-.42	-.30	-.11	.17	.60	1.10	1.61	2.15	2.70
100	92	3.22	3.71	4.14	4.50	4.76	4.80	4.73	4.46	3.60	1.09	.79	.79	.79	.79
101	93	.79	.79	.79											
102	94	-.47	-.47	-.47	-.48	-.47	-.44	-.36	-.22	.01	.39	.87	1.39	1.94	2.50
103	95	3.04	3.54	3.97	4.34	4.59	4.68	4.66	4.47	3.69	1.31	.97	.97	.97	.97
104	96	.97	.97	.97											
105	97	-.47	-.47	-.47	-.48	-.47	-.46	-.41	-.30	-.09	.25	.68	1.18	1.72	2.29
106	98	2.85	3.36	3.81	4.19	4.47	4.58	4.59	4.44	3.77	1.53	1.15	1.15	1.15	1.15
107	99	1.15	1.15	1.15											
108	100	-.47	-.47	-.47	-.47	-.47	-.47	-.44	-.35	-.17	.12	.51	.98	1.50	2.07
109	101	2.64	3.17	3.65	4.05	4.35	4.49	4.52	4.39	3.82	1.75	1.32	1.32	1.32	1.32
110	102	1.32	1.32	1.32											
111	103	-.47	-.47	-.47	-.47	-.47	-.49	-.47	-.39	-.23	.01	.34	.78	1.29	1.85
112	104	2.43	2.98	3.48	3.91	4.23	4.39	4.43	4.30	3.84	1.97	1.50	1.20	.71	-.27
113	105	-1.20	-2.29	-3.39											
114	106	-.47	-.47	-.47	-.47	-.47	-.48	-.49	-.46	-.40	-.30	-.13	.16	.56	1.07
115	107	1.63	2.22	2.76	3.21	3.54	3.74	3.82	3.79	3.65	2.79	2.20	1.75	1.19	.24
116	108	-.70	-1.77	-2.85											
117	109	-.47	-.47	-.47	-.47	-.47	-.47	-.47	-.47	-.47	-.44	-.37	-.22	.02	.38
118	110	.83	1.36	1.91	2.39	2.77	3.01	3.15	3.18	3.18	3.11	2.78	2.27	1.67	.74
119	111	-.17	-1.25	-2.33											
120	112	-.47	-.47	-.47	-.47	-.47	-.47	-.47	-.48	-.48	-.48	-.45	-.42	-.31	-.14

121	113	.13	.54	1.02	1.53	1.99	2.31	2.54	2.64	2.71	2.83	2.91	2.69	2.15	1.25
122	114	.32	-.74	-1.81											
123	115	-.47	-.47	-.47	-.47	-.47	-.47	-.47	-.47	-.47	-.47	-.47	-.47	-.45	-.41
124	116	-.29	-.06	.27	.70	1.17	1.60	1.96	2.19	2.36	2.52	2.70	2.81	2.55	1.74
125	117	.81	-.24	-1.29											
126	118	-.47	-.47	-.47	-.47	-.47	-.47	-.47	-.47	-.47	-.47	-.47	-.47	-.46	-.46
127	119	-.42	-.35	-.22	.06	.43	.92	1.40	1.77	2.06	2.23	2.36	2.52	2.57	2.12
128	120	1.29	.26	-.79											
129	121	-.47	-.47	-.47	-.47	-.47	-.47	-.47	-.47	-.47	-.47	-.47	-.47	-.47	-.47
130	122	-.47	-.45	-.39	-.26	-.03	.34	.77	1.23	1.64	1.89	2.05	2.16	2.24	2.22
131	123	1.70	.75	-.30											
132	124	-.47	-.47	-.47	-.47	-.47	-.47	-.47	-.47	-.47	-.47	-.47	-.47	-.47	-.47
133	125	-.47	-.47	-.44	-.40	-.30	-.10	.19	.59	1.01	1.31	1.53	1.65	1.74	1.89
134	126	1.84	1.18	.19											
135	127	-.47	-.47	-.47	-.47	-.47	-.47	-.47	-.47	-.47	-.47	-.47	-.47	-.47	-.47
136	128	-.48	-.48	-.47	-.47	-.43	-.37	-.23	.01	.30	.59	.85	1.01	1.15	1.33
137	129	1.50	1.41	.65											
138	130	-.48	-.48	-.48	-.48	-.48	-.48	-.48	-.48	-.48	-.48	-.48	-.48	-.48	-.48
139	131	-.48	-.48	-.48	-.48	-.48	-.47	-.44	-.35	-.21	-.02	.20	.39	.57	.74
140	132	.93	1.15	.97											
141	133	-.48	-.48	-.48	-.48	-.48	-.48	-.48	-.48	-.48	-.48	-.48	-.48	-.48	-.48
142	134	-.48	-.48	-.48	-.48	-.48	-.48	-.47	-.46	-.43	-.35	-.24	-.09	.07	.22
143	135	.41	.66	.86											
144	136	-.49	-.49	-.49	-.49	-.49	-.49	-.49	-.49	-.49	-.49	-.49	-.49	-.49	-.49
145	137	-.49	-.49	-.49	-.49	-.49	-.49	-.49	-.49	-.49	-.47	-.43	-.35	-.26	-.15
146	138	-.01	.20	.43											
147	139	-.50	-.50	-.50	-.50	-.50	-.50	-.50	-.50	-.50	-.50	-.50	-.50	-.50	-.50
148	140	-.50	-.50	-.50	-.50	-.50	-.50	-.50	-.50	-.50	-.50	-.49	-.47	-.43	-.37
149	141	-.28	-.14	.03											
150	142	-.51	-.51	-.51	-.51	-.51	-.51	-.51	-.51	-.51	-.51	-.51	-.51	-.51	-.51
151	143	-.51	-.51	-.51	-.51	-.51	-.51	-.51	-.51	-.51	-.52	-.52	-.52	-.50	-.48
152	144	-.44	-.36	-.26											
153	145	-.53	-.53	-.53	-.53	-.53	-.53	-.53	-.53	-.53	-.53	-.53	-.53	-.53	-.53
154	146	-.53	-.53	-.53	-.53	-.53	-.53	-.53	-.53	-.53	-.53	-.53	-.53	-.53	-.53
155	147	-.51	-.49	-.43											
156	148	-.55	-.55	-.56	-.56	-.56	-.56	-.56	-.56	-.56	-.56	-.56	-.56	-.56	-.56
157	149	-.55	-.56	-.56	-.56	-.56	-.56	-.56	-.56	-.56	-.56	-.56	-.56	-.56	-.56
158	150	-.55	-.55	-.53											
159	151	-.61	-.61	-.61	-.61	-.61	-.61	-.61	-.61	-.61	-.61	-.61	-.61	-.61	-.61
160	152	-.61	-.61	-.61	-.61	-.61	-.61	-.61	-.61	-.61	-.61	-.61	-.61	-.61	-.61
161	153	-.61	-.60	-.60											

Printed in the United States of America. Available from  
National Technical Information Service  
U.S. Department of Commerce  
5285 Port Royal Road  
Springfield, VA 22161

Microfiche \$3.00

001-025	4.00	126-150	7.25	251-275	10.75	376-400	13.00	501-525	15.25
026-050	4.50	151-175	8.00	276-300	11.00	401-425	13.25	526-550	15.50
051-075	5.25	176-200	9.00	301-325	11.75	426-450	14.00	551-575	16.25
076-100	6.00	201-225	9.25	326-350	12.00	451-475	14.50	576-600	16.50
101-125	6.50	226-250	9.50	351-375	12.50	476-500	15.00	601-up	

Note: Add \$2.50 for each additional 100-page increment from 601 pages up.

LAST  
REPORT LIBRARY  
SEP -5 1980  
RECEIVED